RI 9536

REPORT OF INVESTIGATIONS/1995

Improved Performance of Linear Coal Cutting Compared With Rotary Cutting

UNITED STATES DEPARTMENT OF THE INTERIOR

UNITED STATES BUREAU OF MINES

U.S. Department of the Interior Mission Statement

As the Nation's principal conservation agency, the Department of the Interior has responsibility for most of our nationally-owned public lands and natural resources. This includes fostering sound use of our land and water resources; protecting our fish, wildlife, and biological diversity; preserving the environmental and cultural values of our national parks and historical places; and providing for the enjoyment of life through outdoor recreation. The Department assesses our energy and mineral resources and works to ensure that their development is in the best interests of all our people by encouraging stewardship and citizen participation in their care. The Department also has a major responsibility for American Indian reservation communities and for people who live in island territories under U.S. administration.

Report of Investigations 9536

Improved Performance of Linear Coal Cutting Compared With Rotary Cutting

By W. W. Roepke, B. D. Hanson, R. C. Olson, C. F. Wingquist, and T. A. Myren

UNITED STATES DEPARTMENT OF THE INTERIOR
Bruce Babbitt, Secretary

BUREAU OF MINES
Rhea L. Graham, Director

International Standard Serial Number
ISSN 1066-5552

CONTENTS

ILLUSTRATIONS

ILLUSTRATIONS—Continued

TABLES

UNIT OF MEASURE ABBREVIATIONS USED IN THIS REPORT

cm	centimeter	lb	pound
cm/s	centimeter per second	m	meter
deg	degree	m^3/min	cubic meter per minute
ft	foot	mg/m^3	milligram per cubic meter
ft^3/min	cubic foot per minute	min	minute
g	gram	ms	millisecond
g/m	gram per meter	N	newton
gpm	gallon per minute	N-m	newton-meter
hp	horsepower	oz	ounce
in	inch	pct	percent
in/s	inch per second	rpm	revolution per minute
kg	kilogram	μm	micrometer
kN	kilonewton	°C	degree Celsius
kW	kilowatt	°F	degree Fahrenheit
L/min	liter per minute		

IMPROVED PERFORMANCE OF LINEAR COAL CUTTING COMPARED WITH ROTARY CUTTING

By W. W. Roepke,[1] B. D. Hanson,[2] R. C. Olson,[3] C. F. Wingquist,[4] and T. A. Myren[5]

ABSTRACT

The linear cutting system, developed by the U.S. Bureau of Mines, uses geometric principles developed by Cardan to produce a nearly constant cut depth. The new system has been extensively tested in a synthetic material under laboratory conditions to verify mechanical capability and to identify operational characteristics.

Comparisons between 15-rpm linear cutting and 50-rpm rotary cutting systems show significant improvement in respirable dust entrainment, product size distribution, and energy usage. Respirable dust is reduced by as much as 90 pct. Recovered product showed a 67-pct reduction in -0.32-cm (-1/8-in) material and a 200-pct increase in +5.08 cm (+2 in) material. Average power was reduced by 66 pct for the linear cutting.

Because the bit cutting paths differ between linear and rotary cutting, it was necessary to compare the two at the same cut depths and bit types. These comparisons show that low revolution per minute rotary cutting entrains about the same amount of respirable dust as the linear cutting system, but the average shaft torque may be 55 to 130 pct greater for the rotary system.

[1]Supervisory physical scientist (retired).
[2]Physical scientist.
[3]Mechanical engineer.
[4]Physical scientist (retired).
[5]Mining engineering technician (retired).
Twin Cities Research Center, U.S. Bureau of Mines, Minneapolis, MN.

INTRODUCTION

The U.S. Bureau of Mines (USBM) at the Twin Cities Research Center in Minneapolis has been working on the prevention and control of airborne respirable dust generation by rotary drum mining machines since enactment of the Federal Coal Mine Health and Safety Act of 1969. The working premise has been "If you don't want dust, don't produce it," but since coal cannot be fragmented without producing dust, practical approaches to the problem have relied on either minimizing the dust generated or control and/or suppression of the dust once it is entrained. While control is adequate to meet near-term regulatory concerns when production is not high, the most economically advantageous approach for either long-term or high-production operations is reduction of the dust generated at the face during the cutting process. This can only be done through redesign of the cutting system. Such a reduction in dust generation would reduce the burden on existing control and suppression techniques allowing the operators to more easily meet the standard. The synergism between a new mining technology and existing control-suppression technology will permit significant increases in production capability.

The USBM has designed a new "linear cutting system" based on geometric principles developed by Cardan in the 1500's. Cardan defined the relationships for a rotating equilateral triangle whose center of rotation also rotates about an eccentric, but in the opposite direction (figure 1). For the case where the center of rotation of the triangle rotates three times for each rotation of the triangle and the radius of the eccentric and the distance from the triangle center to each apex are in the ratio of 9:1, each apex will trace out an approximately square path. The linear cutting system based on this geometry and shown in the artist's rendition of figure 2 consists of a triangular-shaped drum with the bits mounted in a row along each apex. The drum is mounted to a spur gear riding inside a ring gear in such a manner that the triangular drum rotates once for every three rotations of the spur gear inside the ring gear. This gerotor drive system provides a mechanical reduction of 3:1. The cutting concept is described in patent applications (*1-4*).[6]

The development of the linear cutting concept required extensive comparison testing between full-sized linear and rotary-cutting drums to quantify the specific differences between the two cutting systems. This was done in two phases. Initial testing was done to provide proof of concept for the linear system, and to furnish preliminary comparisons with current rotary cutting systems. Based on these results, a more comprehensive test series was conducted to statistically confirm the preliminary findings, to compare the linear cutting system with rotary cutting drums operating with similar bit speeds, and to investigate the cutting parameters associated with the noted reduction in dust. This testing was done using a synthetic material, whose force characteristics closely approximated Illinois No. 6 coal.

Figure 1

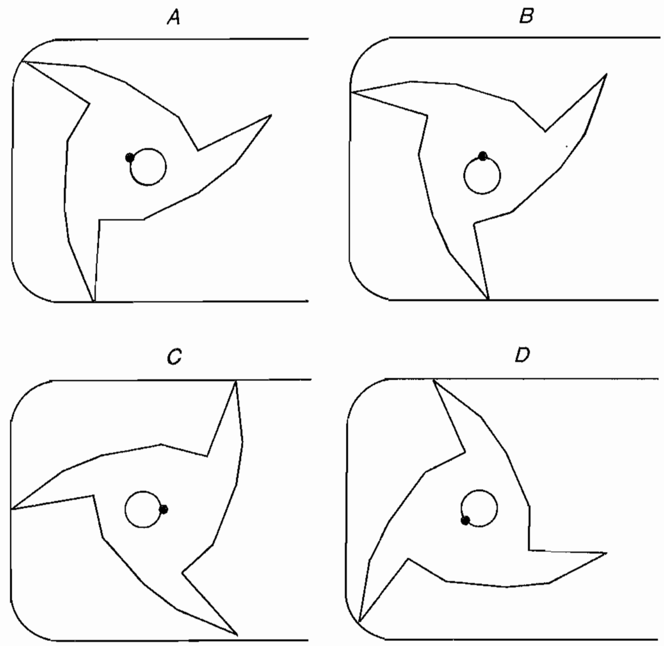

Cutting sequence of linear drum. A, No rotation; B, 45° rotation; C, 135° rotation; D, 270° rotation.

Figure 2

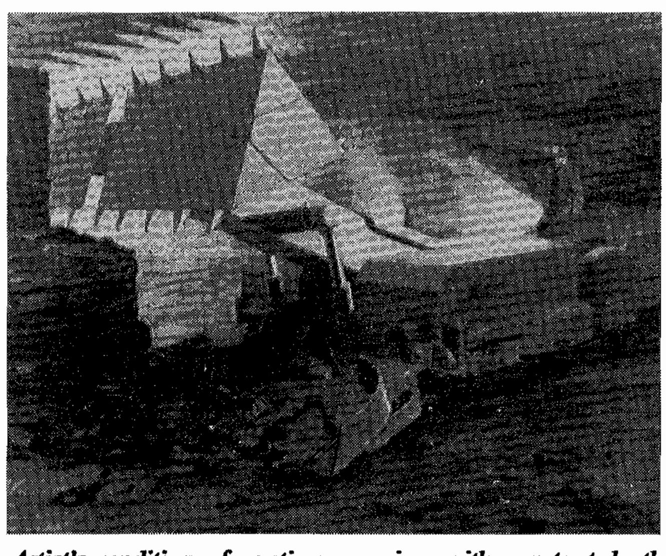

Artist's rendition of continuous miner with constant-depth linear cutter (CDLC) drum.

[6]Italic numbers in parentheses refer to items in the list of references preceding the appendixes at the end of this report.

LINEAR CUTTING CONCEPT BACKGROUND

The linear cutting concept was developed from the analyses of rotary cutting technology by the USBM in 1976 (*5*). These investigations related the depth of cut for each bit on the drum to the dust and forces generated per unit volume of coal cut. With rotary cutting each bit on the drum enters the coal face at zero depth of cut. As the bit proceeds in its circular path the depth of cut increases to a maximum at the horizontal centerline. Once the bit is past the centerline the depth of cut decreases until the bit exits at zero depth (figure 3A). The relationship between the depth of cut and the volume recovered for rotary cutting is shown in table 1.

Table 1.—Change in volume recovery with changing depth of cut for rotary drum

Pct of rotation	Pct of maximum cut depth	Pct of total volume removed
10	18.4	1.7
20	33.4	5.7
30	47.6	11.9
40	60.6	20.2
50	72.1	30.4
60	81.9	42.3
70	89.7	55.5
80	95.4	69.8
90	98.8	86.6
100	100.0	100.0

Figure 3

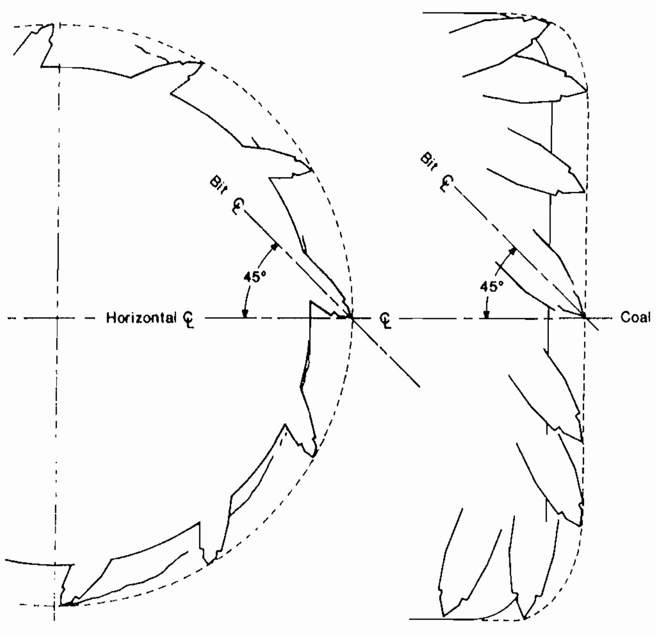

Schematic comparison of bit paths for rotary (A) and CDLC (B) miners.

It can be seen that the cutting action between zero and approximately 75 pct of maximum depth of cut produces about one-third of the total volume of coal recovered. That portion of the cut constitutes the shallow-cutting, low-coal-recovery part of the drum rotation where the ratio of dust produced and energy used to the volume recovered is maximum. It follows that if one wishes to design an improved cutting system, the low-recovery portion of the rotary cut must be eliminated from the system to minimize the ratio of dust and energy to volume recovered.

Figure 3B shows the reduction in the amount of shallow cutting by a linear drum as compared with a rotary drum. Table 2 shows the relationship between depth of cut and volume removed for the linear drum. Figure 4 shows the comparison between rotary and linear cutting. When both drums have reached 75 pct of maximum cut depth, the rotary drum has removed approximately 33 pct of the total volume. The linear drum has taken only 15 pct in this shallow cutting region. The linear drum takes approximately 70 pct of the total volume at cut depths between 95 and 100 pct of its maximum depth of cut. The rotary drum removes only 30 pct in this range of cut depths. The linear drum not only cuts less material at shallow depths of cut, but also does 70 pct of its cutting at or near the maximum cut depth.

Table 2.—Change in volume recovery with changing depth of cut for linear drum

Pct of rotation	Pct of maximum cut depth	Pct of maximum volume recovered
10	12.7	0.9
20	30.7	3.8
30	59.5	9.8
40	86.2	19.8
50	97.2	32.4
60	99.7	45.8
70	100	59.3
80	100	72.9
90	100	86.4
100	100	100

Rotary drums create an additional problem by generating secondary dust, which may be substantially greater than any primary dust generation due to cutter action. It has been said that: "...using blunt, high-speed bits, (continuous mining machines) probably are the best machines for forming dust that could be invented, except for a grinding stone" (*6*). This has been substantiated by Matta (*7*) who has shown that a continuous miner produces 70 pct of the total dust while sumping, and only 20 pct while shearing. The remaining 10 pct is attributed to gathering and loading. These differences in dust values

Figure 4

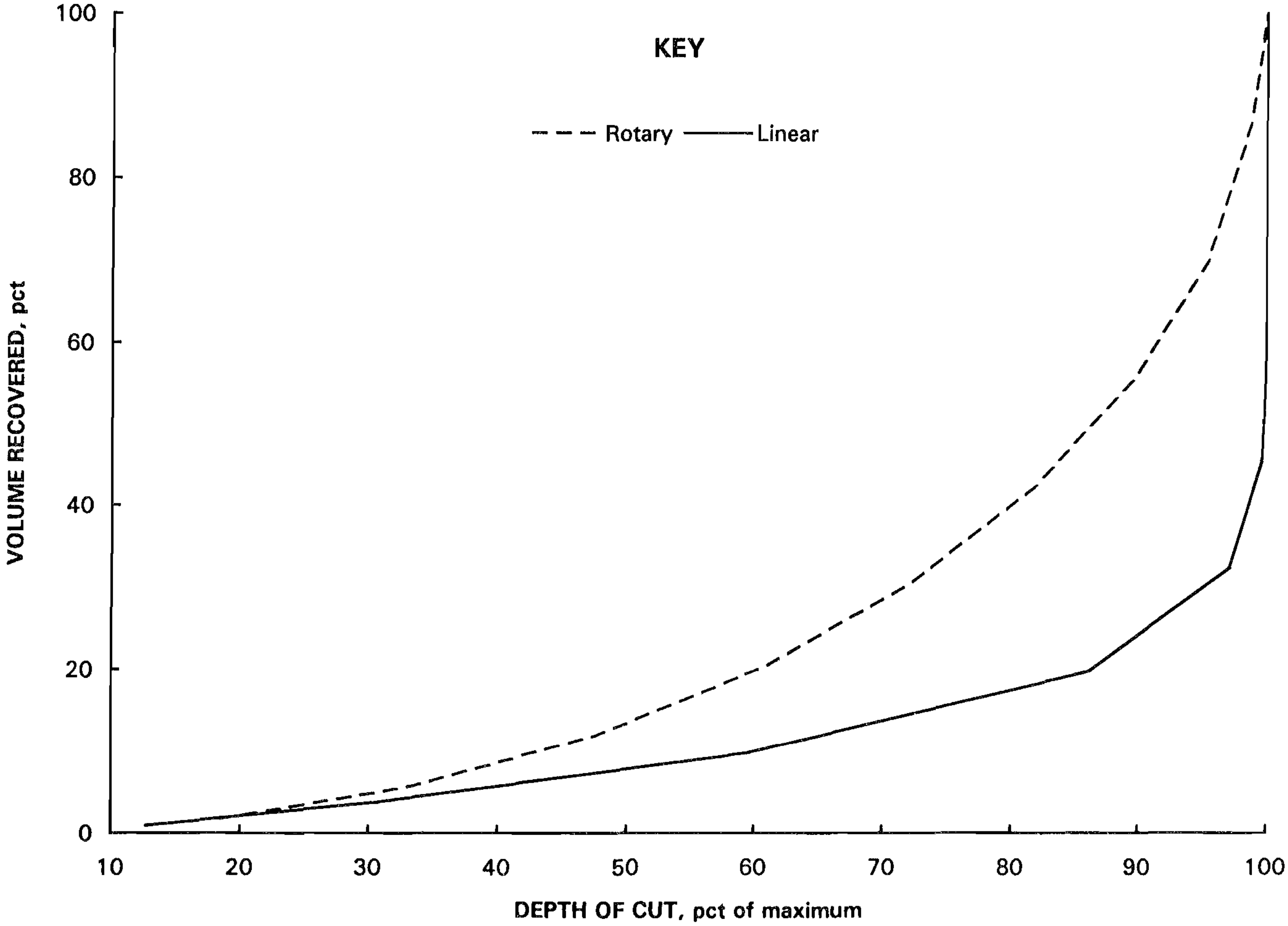

Volume removed versus cut depth for linear and rotary drums.

between sump and shear for a continuous miner may be attributed to (1) less breakout of the coal to a free face on sump than shear, and (2) the grinding action of the drum head on fragmented coal caught between the drum and the face before discharge during sump cutting. These differences suggest that one way to significantly reduce dust generation is to reduce regrinding by eliminating the sumping action and/or by cutting to an open face at all times.

Identification of the sumping action of continuous miners as the highest dust generation source at the face, lends insight into the dust generation problems for longwall shearers. The sump portion of continuous mining is equivalent to a longwall shearer advancing along the face. Even though they are called shearers, longwall shearers cut only with a full-drum diameter, or in continuous miner parlance, "on sump." The only time a shearer does not cut in sump is with the trailing drum on a double-drum shearer or a return cleanup pass with a single-drum shearer. This means that any longwall shearer will constantly cut in the highest dust generation mode with the lead drum. The linear cutting concept does not eliminate sumping action, but it does modify the cutting action so the drum will be cutting to an open face most of the time with minimal secondary fragmentation.

LINEAR CUTTING SYSTEM DESIGN

The development of the linear cutting concept required the design of a gerotor gearbox to provide linear cutting action of the head. The internal working parts of the gerotor gearbox are shown in figure 5. Inside the drum is an eccentrically mounted drive shaft with a 5.08-cm (2-in) offset. A large spur gear with 8.9-cm-long (3.5-in) cycloidal shaped teeth is mounted on the shaft. This gear is directly connected to the cutting drum and is free to rotate about the shaft. The drive shaft drives the spur gear inside a stationary ring gear. This ring gear has teeth that are 2.54-cm-diameter (1-in) cylinders that can rotate freely around a mounting pin as the spur gear engages them. There are 16 cylinders and 12 gear teeth that give the 3 to 1 reduction ratio of the mechanism. Since this is a single-stage reduction, the output rotates in an opposite direction of the input. The centerline of the eccentric shaft and spur gear will rotate counterclockwise around the input drive when viewed from the end of cutting drum. The drum and spur gear rotate in a clockwise direction on the shaft. To have proper geometry for linear motion, the drum radius, i.e., centerline to bit tip, must be approximately nine times the offset, or 45.72 cm (18 in) for the prototype head shown here.

INITIAL CONCEPT VERIFICATION

The purpose of the initial testing was to determine the mechanical viability of the gerotor drive system. This testing had to confirm that the gearbox could make the triangular drum cut a square face and would be able to handle any high-torque loads which may be encountered.

Figure 5

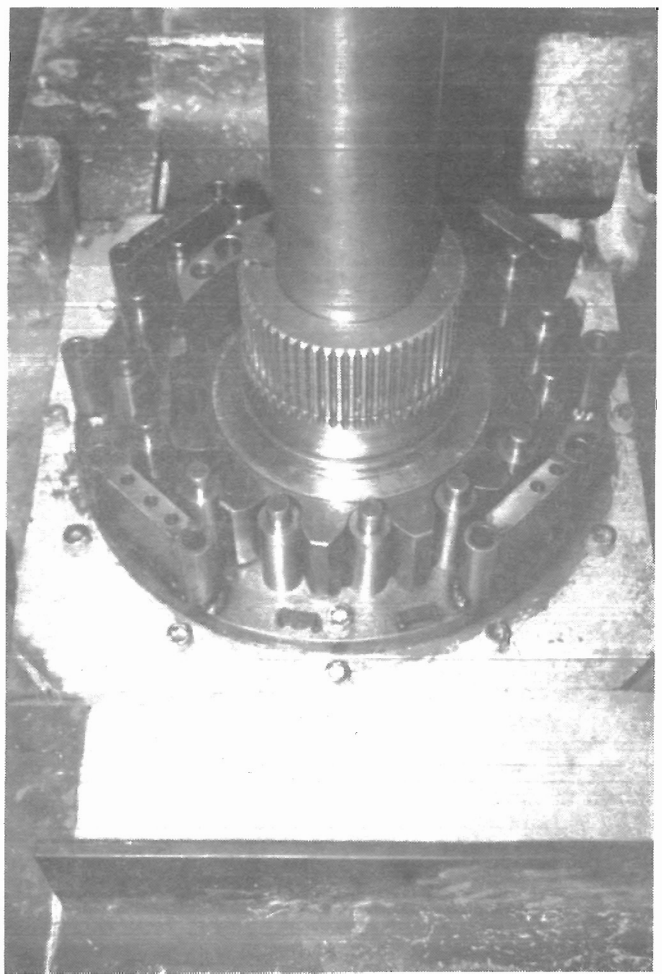

Internal gearbox.

The initial linear drum, shown at the rear top of figure 6, has three rows of forward attack bits set laterally along each apex of the triangular-shaped drum with each row radially spaced 120° apart. Seventeen chisel-type cutter bits are mounted on the drum with six, six, and five bits per row. In each row the bit spacing is 15.24 cm (6 in) apart with each set offset by 5.08 cm (2 in), so the line spacing is 5.08 cm (2 in). The bits are 1.91 cm (3/4 in) wide. This drum is referred to in the text as L1. L1 was tested at 10 rpm and a 0.64-cm/s (0.25-in/s) infeed rate. The initial rotary drum had two vanes and was laced with commercially available conical bits welded to the vanes without any bit blocks. Since bit wear was not considered a problem due to the limited testing, there was no need for bit rotation. The lacing was 7.62 cm (3 in) between bits on each vane, but the bits were offset on the second vane by 3.81 cm (1½ in), so the line spacing between vanes was 3.81 cm (1½ in). This drum is referred to in the text as R1. As comparison, the R1 rotary drum was tested at the same 0.64 cm/s (0.25 in/s) infeed rate, but at a more typical drum speed of 50 rpm. These tests were conducted in a synthetic material. A description of the synthetic material and the test facility is in appendix A.

The results (figure 7) show a reduction of better than 90 pct for respirable dust. The torque, thrust, and power required by the linear cutting during these initial tests were between 30 and 65 pct lower than the rotary drum. Comparison of the screened product indicates an average decrease of better than 65 pct for the -0.32-cm (-1/8-in)

Figure 6

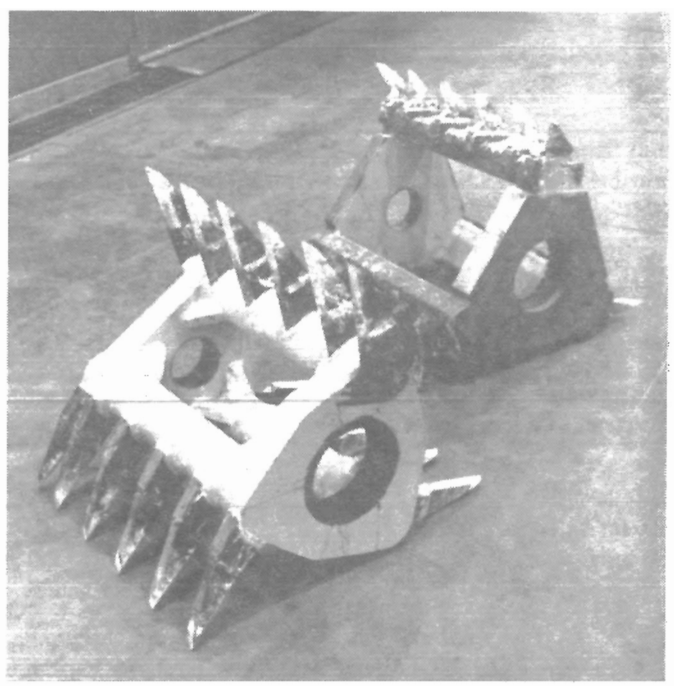

First (upper right) and second (lower left) generation linear cutting drums.

Figure 7

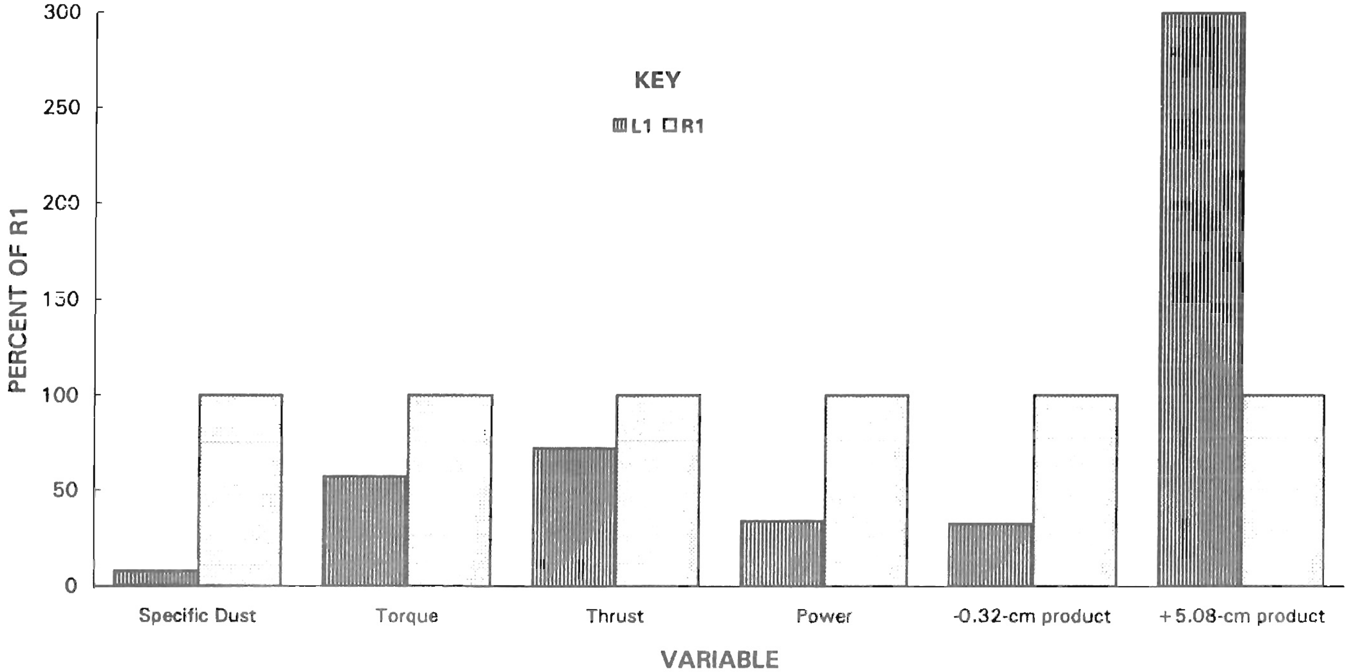

Comparison of L1 linear head and R1 rotary drums.

fines with linear cutting, while the +5.08 cm (+2-in) product showed a better than 200 pct increase. The validity of the new linear cutting concept was fully confirmed by these initial, shallow cutting tests. A summary of the results for these initial tests is shown in table 3.

Table 3.—Summary of comparative results for L1 drum versus R1 drum

Head type	R1 at 50 rpm and 0.64 cm/s infeed rate	L1 at 10 rpm and 0.64 cm/s infeed rate	Pct change
Maximum cut depth, cm .	0.4	1.27	233
Power, kW	37.0	12.5	-66
Thrust, N	11,441	8242	-28
Torque, N-m	7003	4000	-43
Specific dust, mg/m^3	0.485	0.038	-92
+5.08-cm product	8.8	26.4	200
-0.32-cm product	23.0	7.5	-67

COMPARISON TESTING WITH SECOND GENERATION DRUM

Experimental Plan

An expanded set of tests were run to determine any specific differences between standard rotary cutting drums and the linear cutting drum. The second generation linear drum, L2, was compared with the three rotary drums shown in figure 8. These three drums were tested at a drum speed of 50 rpm. The linear drum was tested at a drum speed of 15 rpm. Additionally, the rotary drum, R2A, laced with the forward attack bits was tested at 22 rpm. At this set of operating parameters, the linear drum and the rotary drum would be cutting at the same maximum cut depth with similar bits. This allows a direct

Figure 8

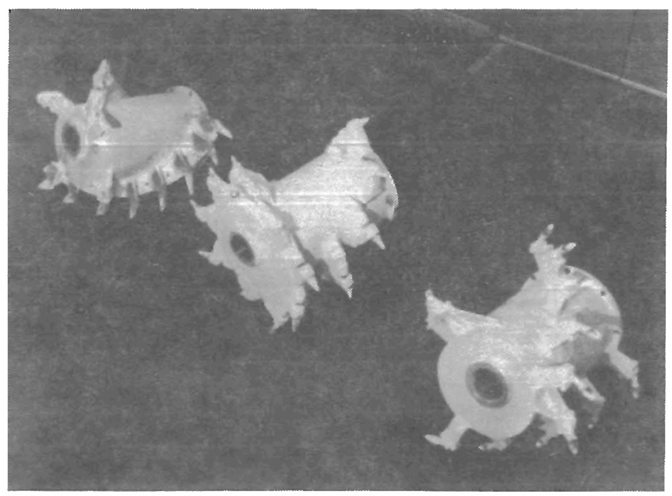

Rotary cutting drums (R2-upper right; R3-center; R4-lower left).

comparison of the two cutting scenarios. All five drums were tested at sample advance rates of 0.95, 1.91, and 2.86 cm/s (0.38, 0.75, and 1.125 in/s). Each of the test conditions was run once.

To quantify the repeatability of the experiment, additional tests were run on a narrower scope. Additional replications of the L2, R2B, and R3 drums were performed at the 1.91 cm/s advance rate. For the L2 and R3 drums two additional tests were run, and for the R2B drum three additional tests were run.

For all of the tests, the total dust generated, distance advanced into the sample block during the test, shaft torque and thrust were measured. The material cut during the tests was also screened to determine the amount passing 0.32 cm (1/8 in) and the amount greater than 5.08 cm (2 in).

Drum Types

The first test series was run at a 0.64-cm/s (0.25-in/s) advance rate. As deeper cuts were attempted with the first linear drum, the material piling at the foot of the face prevented the drum from turning the bottom corner. Owing to the motion of the drum, this material was being compressed by the bit mounting crossbar before the drum could move the piled material out past the backside of the drum. This created an overload condition for the system which activated the automatic shutdown. To solve this problem, a new drum was designed which moved the bit support bar back and added 16.51-cm (6½-in) gauge length to the cutting bits. This increased the free volume for the cut material to accumulate at the foot of the face by 300 pct.

The second generation linear drum, front left of figure 6, has three rows of forward attack bits set along each 30-in apex of the triangular shaped drum 120° apart. The bits are mounted on the drum in the same configuration as the first generation drum, i.e., six, six, and five bits per row. In each set, the bit spacing is 15.24 cm (6 in) apart with each set offset from the previous row by 5.08 cm (2 in), so the line spacing is 5.08 cm (2 in). The bits are 2.54 cm (1 in) wide. This drum is referred to in the text as L2.

The three rotary drums tested (figure 8) are all standard, round, 81.28-cm-diameter (32-in) by 76.2-cm-wide (30 in) types cutting the same size web as the linear drums. The only difference between these drums is in the bit types and lacing.

The first drum at the top of figure 8, is relaced drum R1 with the same forward-attack type bits as L1 welded to the two vanes. This drum is referred to in the text as R2. This drum has 10.16-cm (4-in) bit spacing with a 5.08-cm (2-in) line offset. There are 8 bits on one vane and 9 on the other. Results with this drum, reported for both slow (22½ rpm), and standard speed (50 rpm), are reported in the text as R2A and R2B, respectively.

The middle drum in figure 8 uses a commercially available two-start lacing with conical bits in pedestal mounted blocks. This drum is laced with 12.70-cm (5-in) spacing between bits with a 6.35-cm (2.5-in) offset on the second start so the line spacing between starts is 6.35 cm (2.5 in). There are five bits on each scroll and nine end bits. This drum is referred to in the text as R3.

The bottom drum in figure 8 uses a commercially available three-start lacing with conical bits welded directly to pedestals. This drum is laced with 15.24 cm (6-in) spacing between bits on each start with a 5.08-cm (2-in) offset on subsequent starts so the line spacing between bits is 5.08 cm (2 in). The three scrolls have six, five, and five bits, respectively. This drum is referred to in the text as R4.

Results and Discussion

The test results for the comparison of the linear and the four different rotary configurations are shown in figures 9-16 and table 4. For ease of discussion the data for the linear drum and the three 50 rpm configurations will be discussed separately from the linear drum versus 22.5-rpm drum.

Comparison of Linear Drums and 50-rpm Drums

Figure 9 shows specific dust generated by each drum tested. The linear drum generated less dust than the other three drums, with the greatest difference occurring between the linear drum and the conical bit (R3 and R4) drums. All of the drums, except the R2B drum, showed the characteristic drop in dust levels as the advance rate, and hence, cut depth increased. The R2B and R3 drums cut at an average cut depth approximately one-third (0.357) of the linear drum and the R4 drum cuts at an average cut depth approximately one-quarter (0.238) of the linear drum. This difference in cut depth would explain, in part, the lower dust levels for the linear drum. There also is an apparent difference due to bit type as evidenced by the lower dust levels for the R2B drum which uses forward attack bits and the R3 drum which uses conical bits. For the 2.86 cm/s (1.125 in/s) advance rate with R2B and R3 at 50 rpm, their average cut depth would be roughly equivalent to the linear drum cut depth at the 0.95 cm/s advance rate. In each case, dust levels from the linear drum are lower.

Figure 9

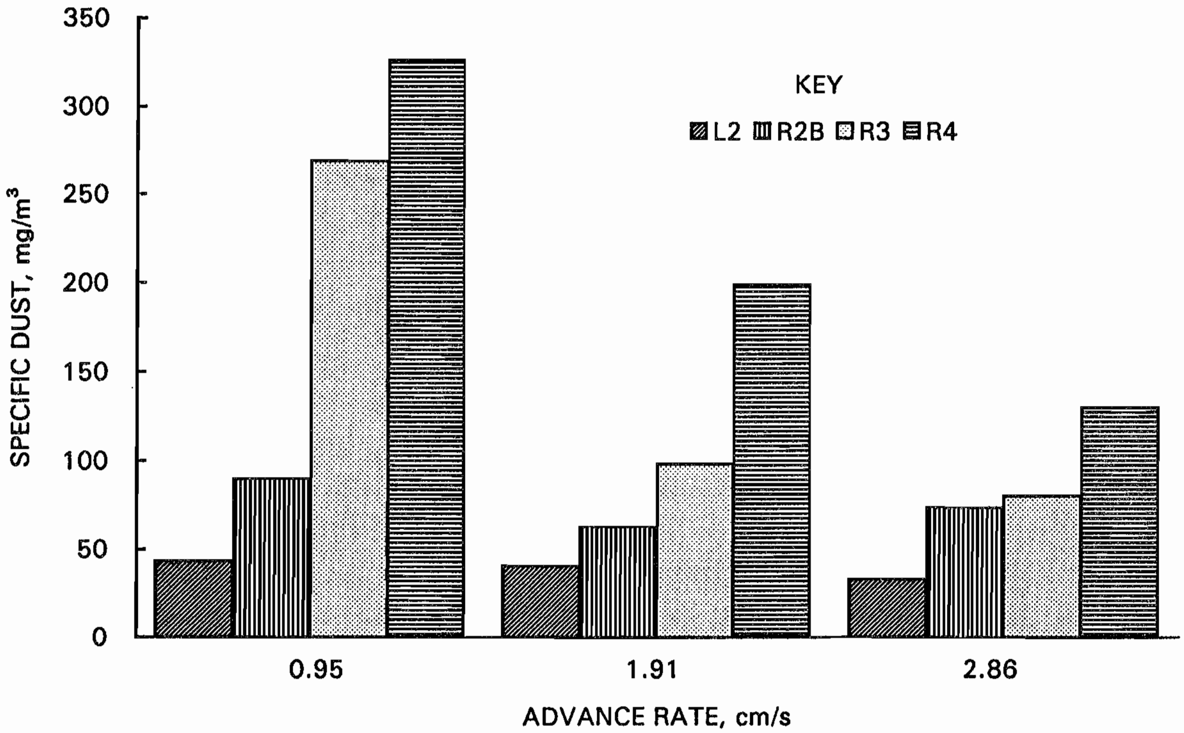

Specific dust results for linear and 50 rpm rotary drums.

Figure 10

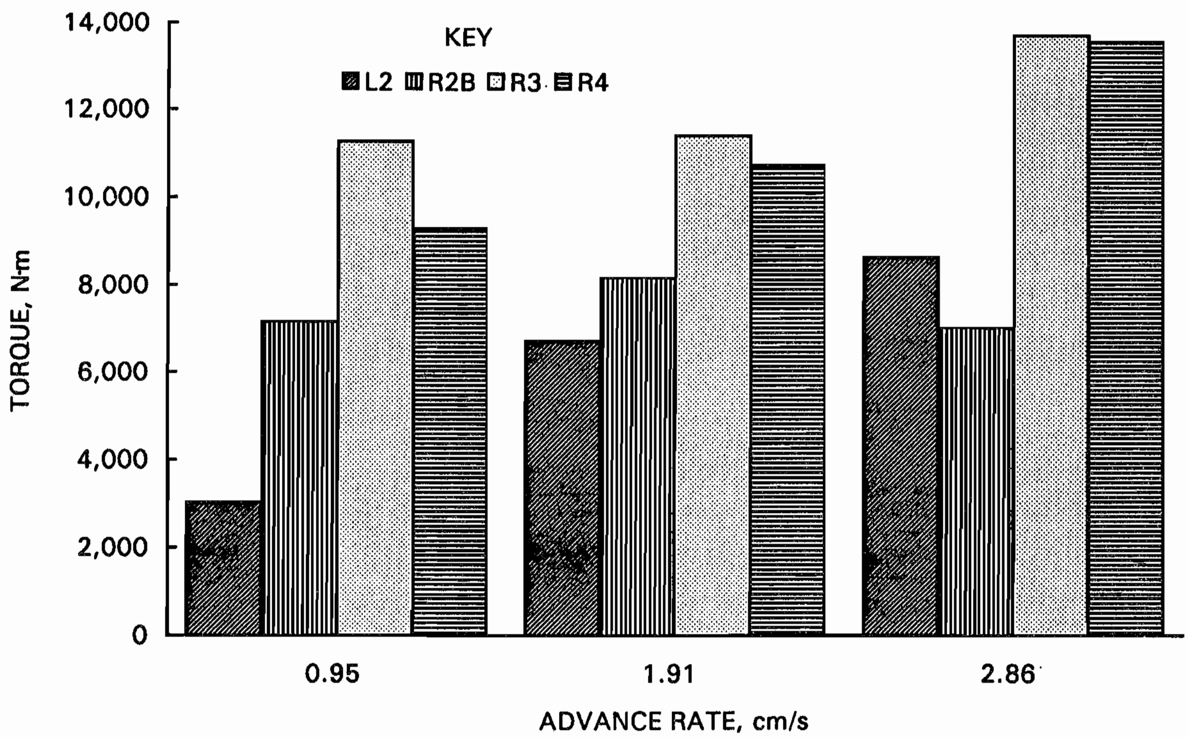

Torque results for linear and 50 rpm rotary drums.

Figure 11

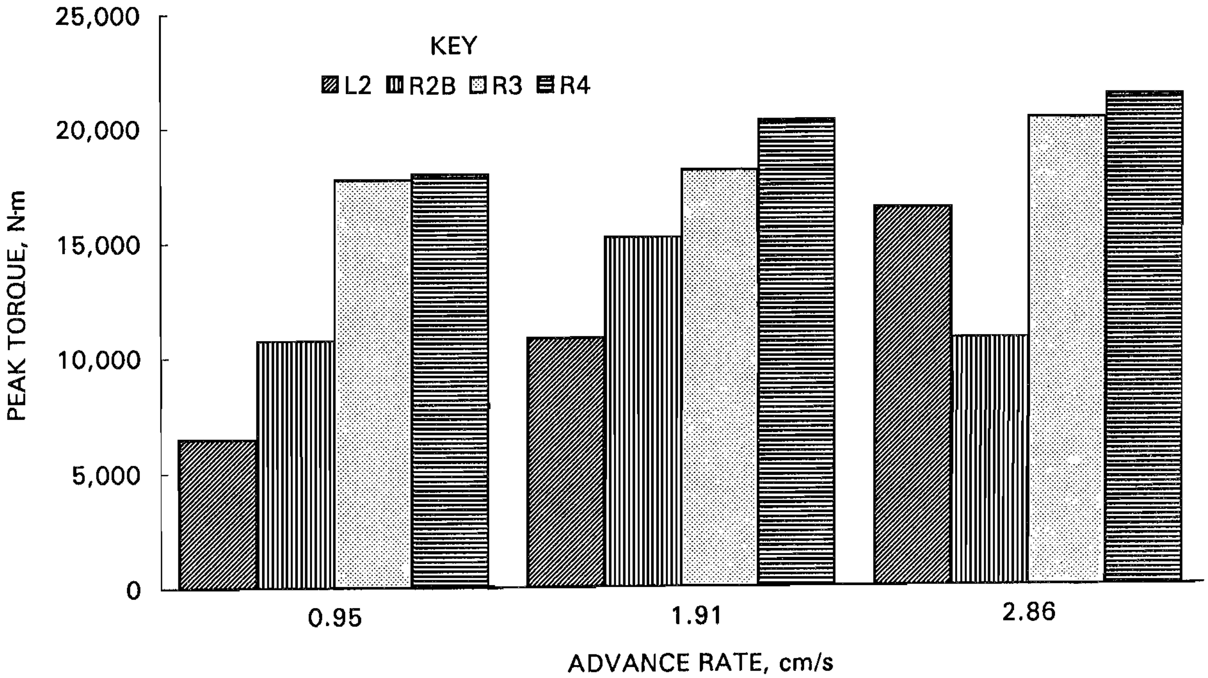

Peak torque results for linear and 50 rpm rotary drums.

Figure 12

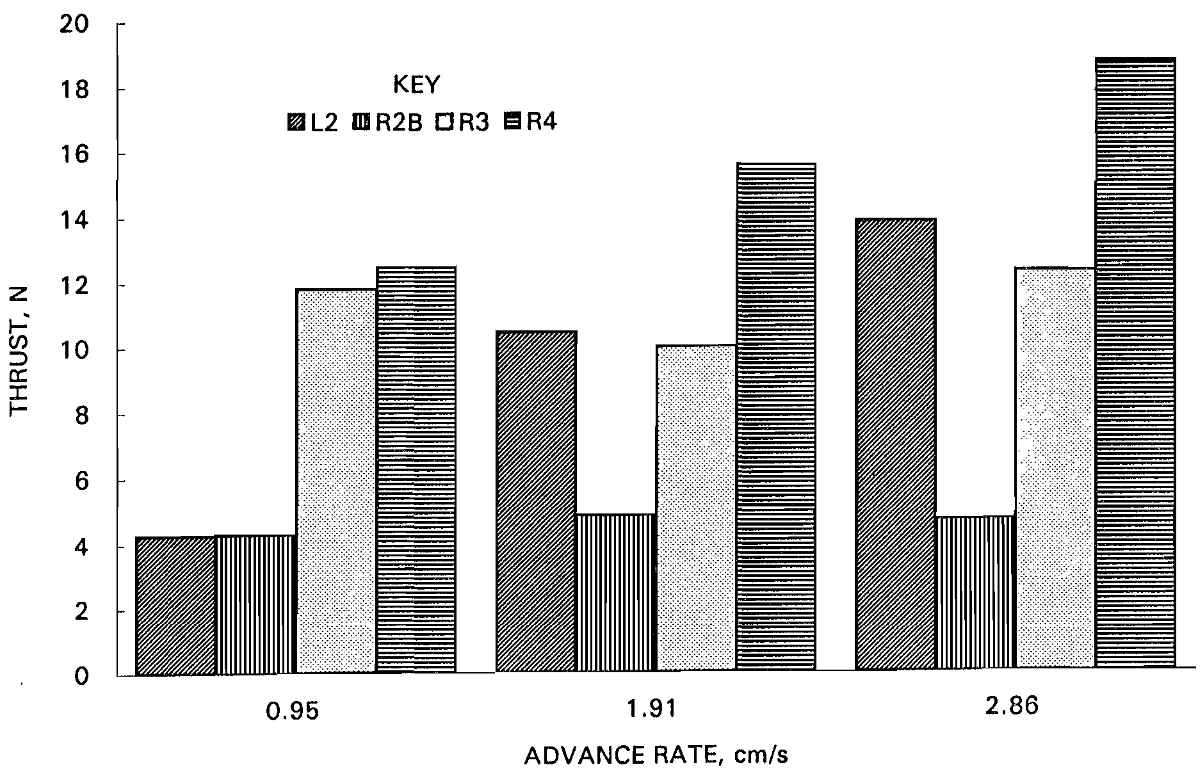

Thrust results for linear and 50 rpm rotary drums.

Figure 13

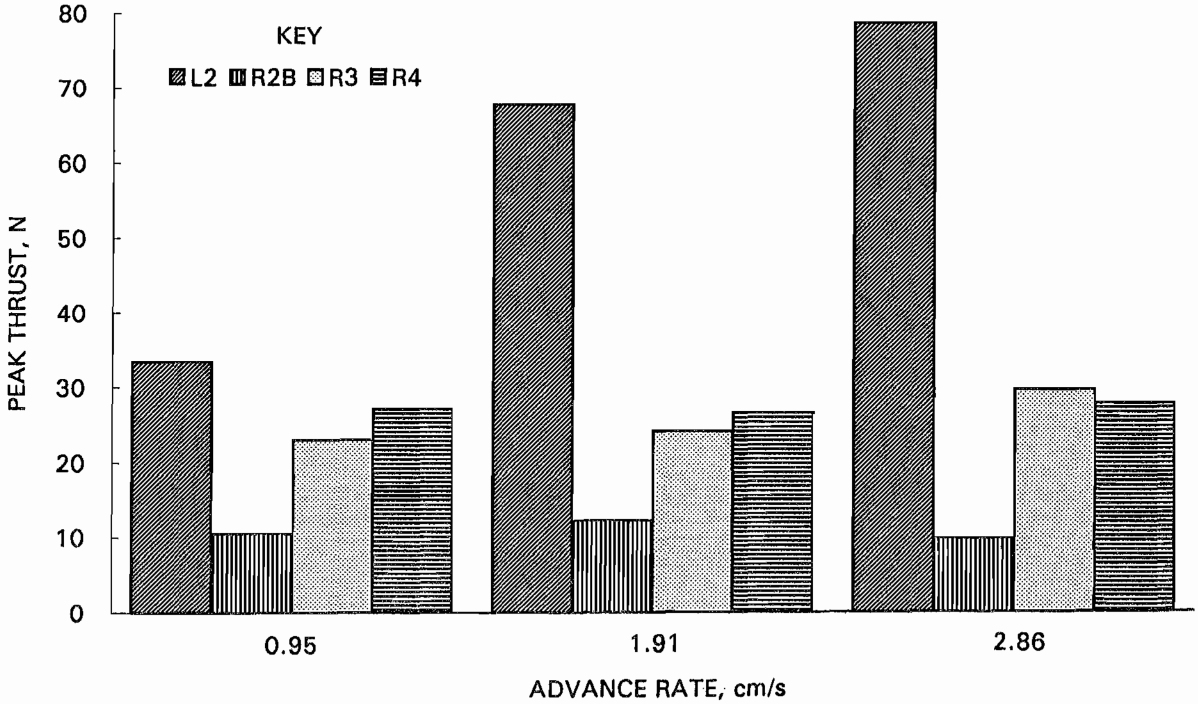

Peak thrust results for linear and 50 rpm rotary drums.

Figure 14

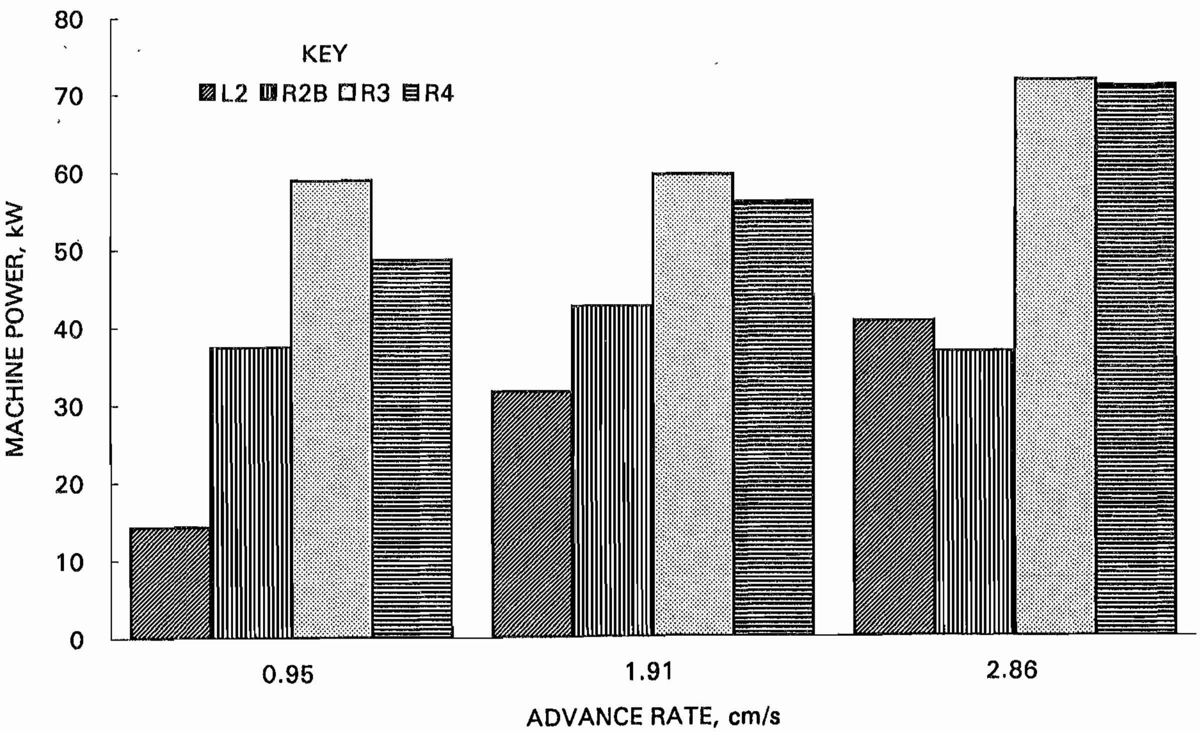

Power results for linear and 50 rpm rotary drums.

Figure 15

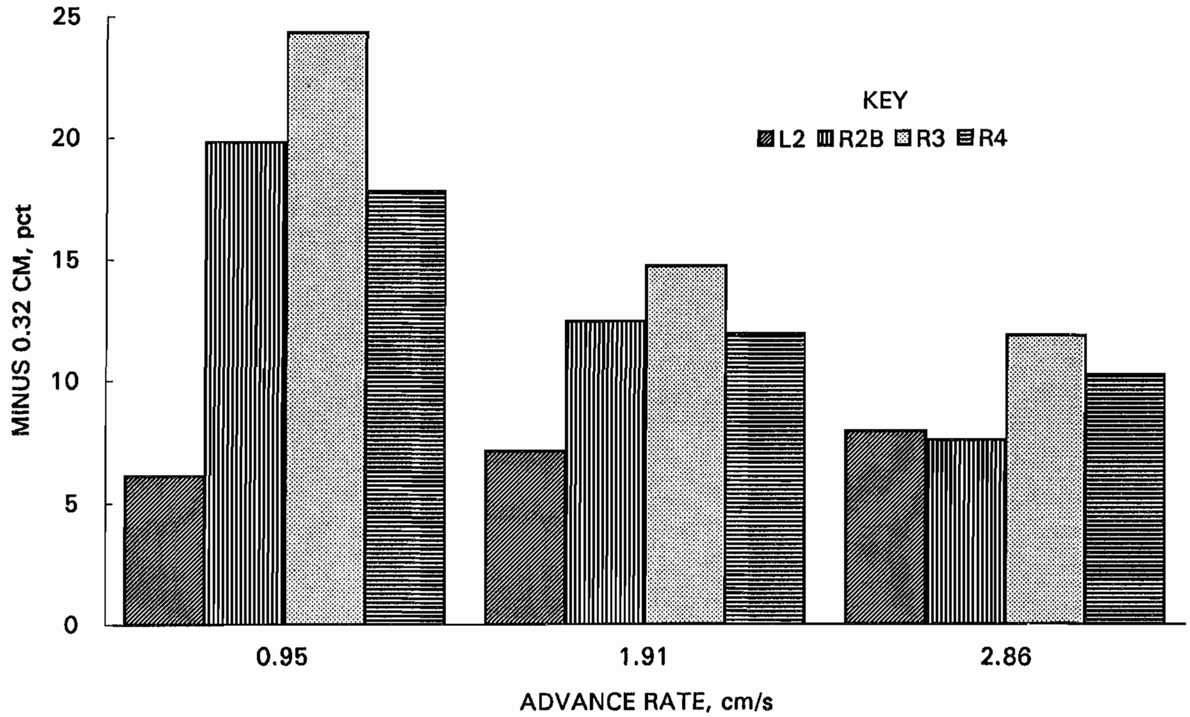

Minus 0.32 cm (1/8 in) results for linear and 50 rpm rotary drums.

Figure 16

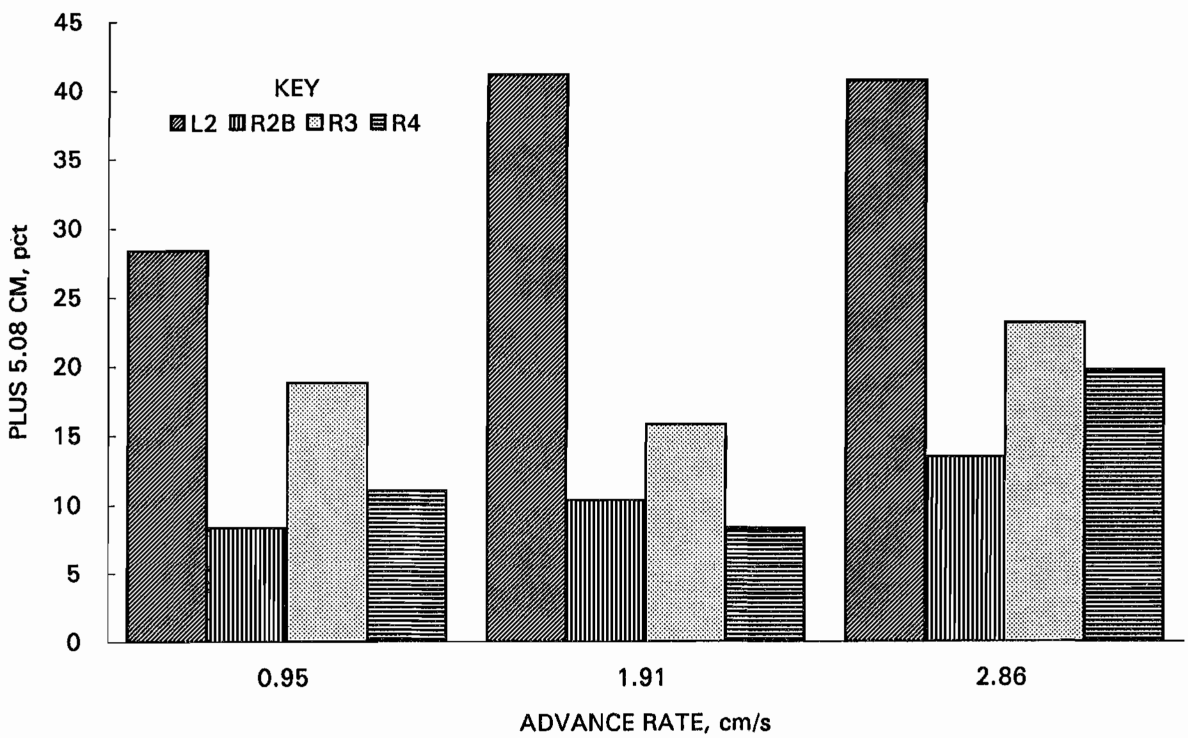

Results for plus 5.08-cm (2-in) material for linear and 50 rpm rotary drums.

Table 4.—Results comparing linear drum and four rotary drum configurations

Variable and drum	Advance rate, cm/s		
	0.95	1.91	2.86
Specific dust, mg/m^3:			
L2	0.035	0.033	0.026
R2A	0.050	0.013	0.009
R2B	0.072	0.050	0.059
R3	0.216	0.078	0.064
R4	0.262	0.159	0.104
Average torque, N-m:			
L2	3,030	6,721	8,624
R2A	6,507	10,434	19,940
R2B	7,153	8,161	7,014
R3	11,263	11,404	13,695
R4	9,291	10,730	13,557
Peak torque, N-m:			
L2	6,459	10,798	16,358
R2A	11,726	16,320	20,873
R2B	10,723	15,161	10,691
R3	17,704	18,066	20,218
R4	17,965	20,203	21,246
Average thrust, kN:			
L2	4.27	10.44	13.78
R2A	4.29	6.27	8.01
R2B	4.29	4.83	4.66
R3	11.80	9.98	12.24
R4	12.47	15.50	18.62
Peak thrust, kN:			
L2	33.4	67.7	78.5
R2A	12.5	16.3	26.8
R2B	10.5	12.1	9.7
R3	23.0	24.0	29.4
R4	27.0	26.5	27.6
Power, kW:			
L2	14.3	31.7	40.6
R2A	15.3	24.6	47.0
R2B	37.5	42.7	36.7
R3	59.0	59.7	71.7
R4	48.7	56.2	71.0
Minus 0.32-cm, pct:			
L2	6.1	7.1	7.9
R2A	6.7	7.9	7.1
R2B	19.8	12.4	7.5
R3	24.3	14.7	11.8
R4	17.8	11.9	10.2
Plus 5.08-cm, pct:			
L2	28.4	41.2	40.7
R2A	15.3	26.6	35.1
R2B	8.3	10.3	13.4
R3	18.8	15.8	23.1
R4	11.0	8.3	19.7

The results for average shaft torque are shown in figure 10. The linear drum was lower in required torque than the conical bit drums with the exception of R2B. Torque increased faster as the advance rate increased for the linear drum than for the rotary drums. The space-depth ratio for the linear drum varies from 4 to 1.3 as the advance rate increases from 0.95 to 2.86 cm/s. The ratio for the rotary drums varies from approximately 13 to 3 or 4 over the same range. If the optimal space-depth ratio for this material is similar to coal (approximately 3) then the rotary drums are approaching their optimal cutting situation as the linear is moving away from its optimal area. This may account for the small changes in torque versus advance rate for the rotary drums. The peak torque values (figure 11) demonstrated the same pattern as the average values.

The results for average thrust (figure 12) were varied. The R2B drum and the linear drum were equal at the 0.95 cm/s advance rate. At the higher advance rate, the R2B drum requires less thrust. The linear drum and R3 drum were approximately equal at the higher advance rates, but the linear drum was lower at the 0.95 cm/s advance rate. Thrust for the linear drum was lower at all three advance rates when compared with the R4 drum. The space-depth ratio would also affect thrust in the same fashion as it does torque. Figure 13 shows the results for peak thrust. The rotary drums followed the same pattern for peak thrust as they did for the average values. The linear drum shows much higher peak thrusts relative to the average values. This is due to the higher thrust experienced in the upper corner as the bit begins its cut.

Figure 14 shows the results for power. The linear drum required fewer kilowatts than the other drums, except for the R2B drum at the 1.125 advance rate.

As evidenced by figure 15, the linear drum also performed better than the other drums in the area of fines produced. The linear drum produced lower amounts of fine material (-0.32 cm or -1/8 in) than the other drums, although the advantage did narrow as the advance rate increased. The amount of coarse material (+5.08 cm or +2 in) was consistently higher for the linear drum (figure 16).

Comparison of Linear Drum and 22-rpm Forward Attack Drum

Table 4 and figures 17-24 show the comparative results between the L2 and R2A drums. The two drums were approximately equal in the amount of specific dust generated (figure 17). Both drums produced considerably lower dust values than the 50 rpm rotary drums. The R2A drum on required higher shaft torque, both average and peak, than the L2 drum (figures 18 and 19). The reverse (figures 20 and 21) was true for average and peak thrust. The drums were roughly equivalent in terms of power (figure 22). The two drums produced approximately the same amount of fines (figure 23). The linear drum produced more 5.08-cm (+2-inch) material (figure 24).

Figure 17

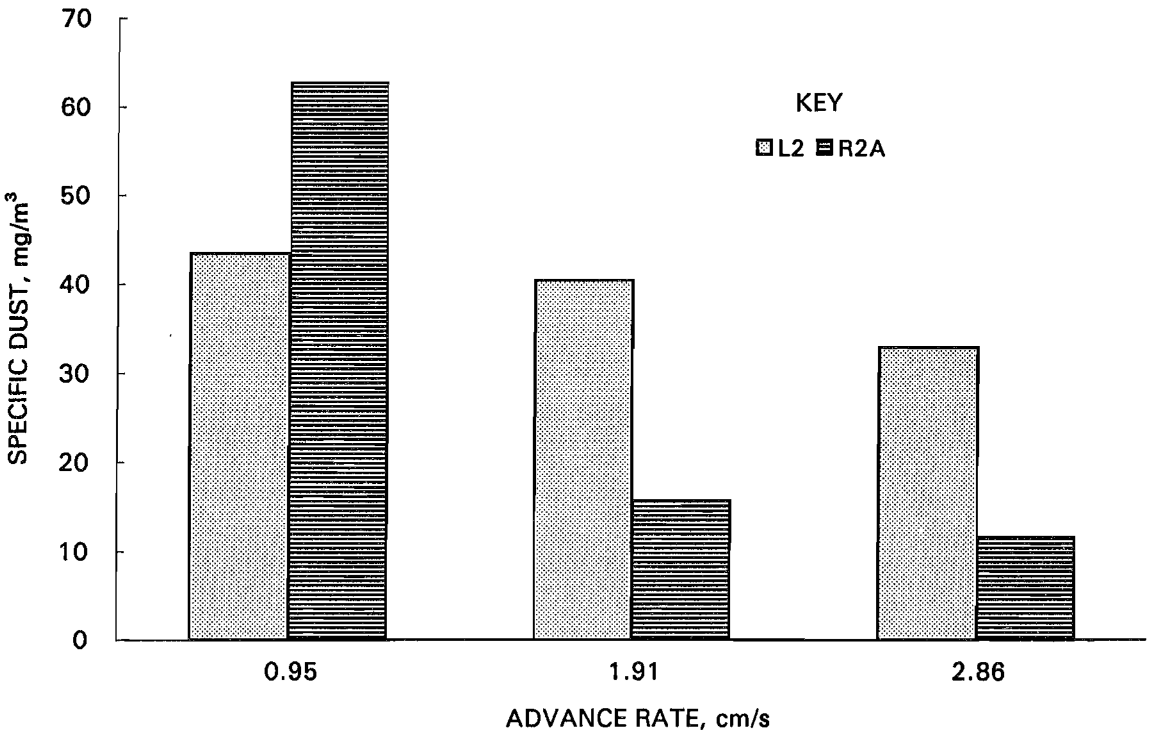

Results for specific dust for linear and slow rotary drum.

Figure 18

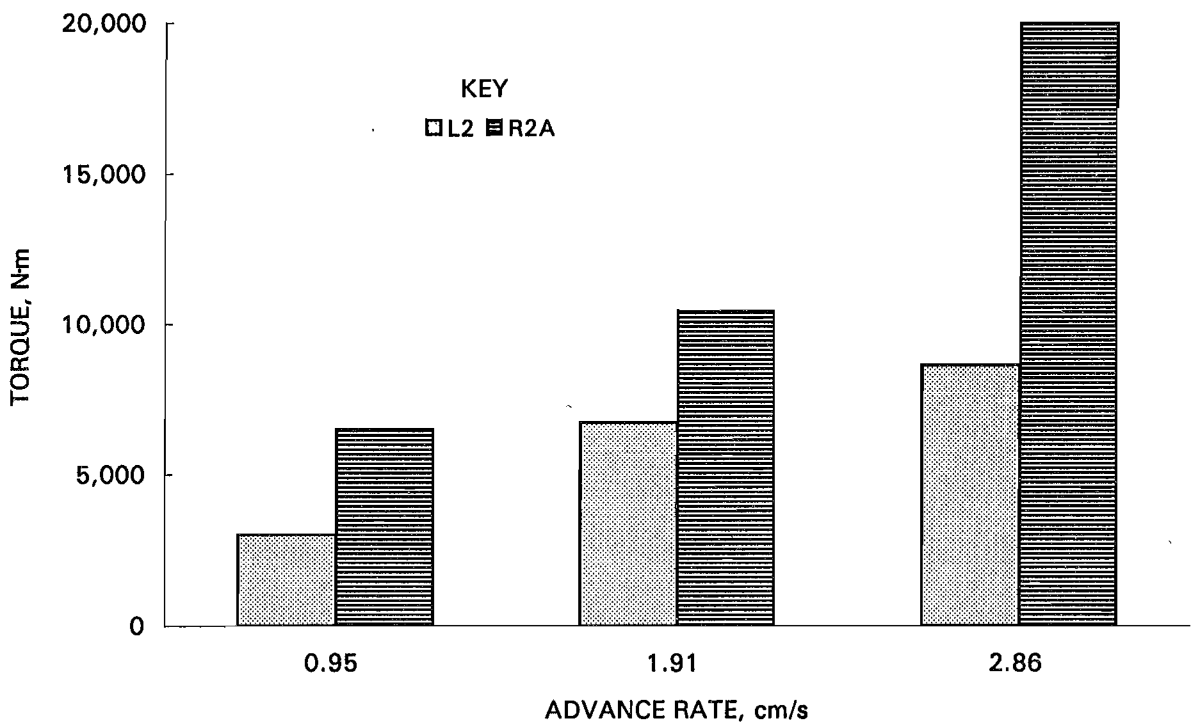

Torque results for linear and slow rotary drum.

Figure 19

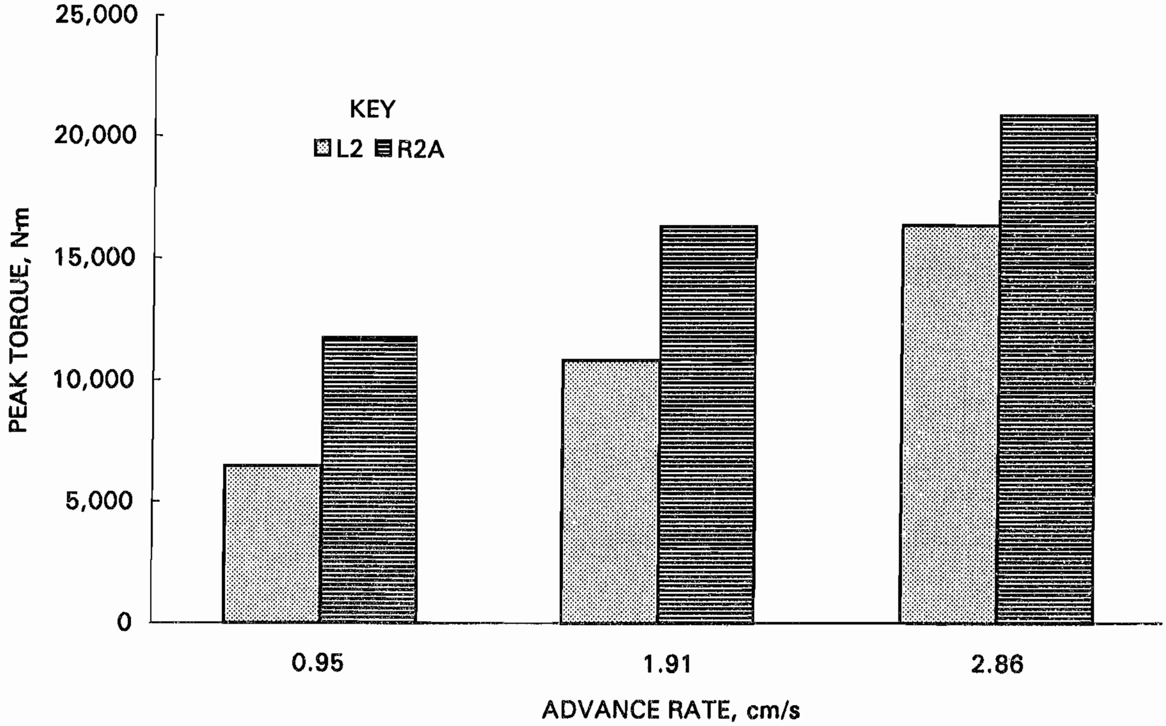

Peak torque results for linear and slow rotary drum.

Figure 20

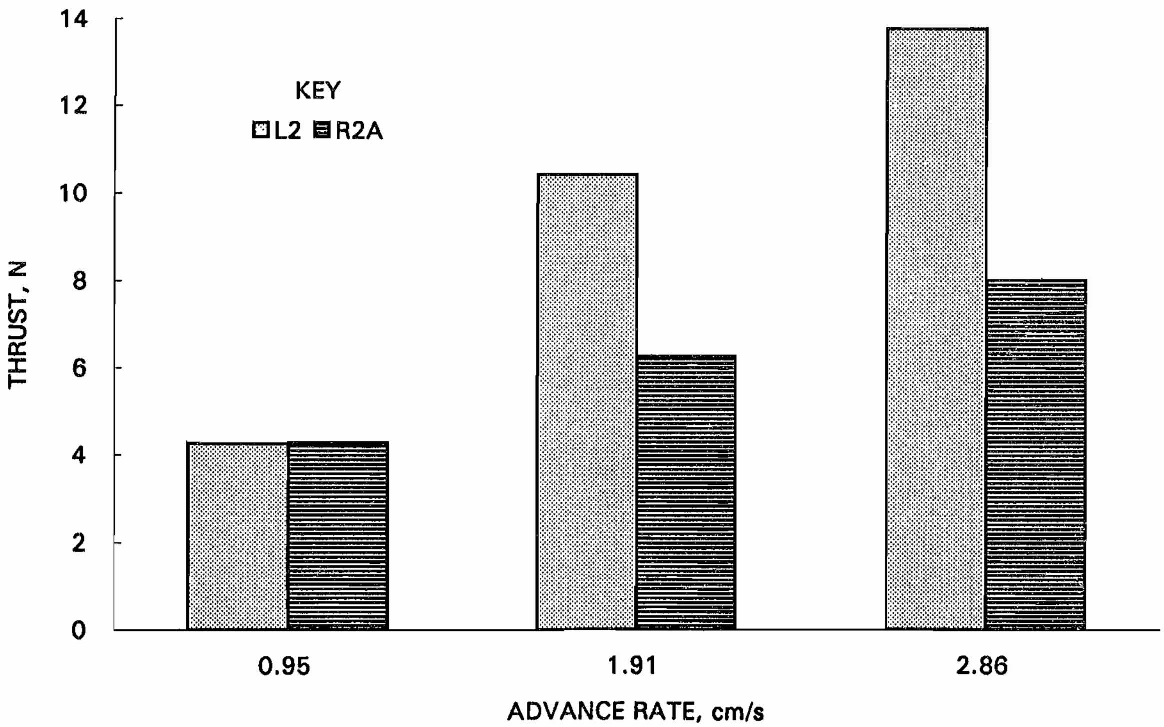

Thrust results for linear and slow rotary drum.

Figure 21

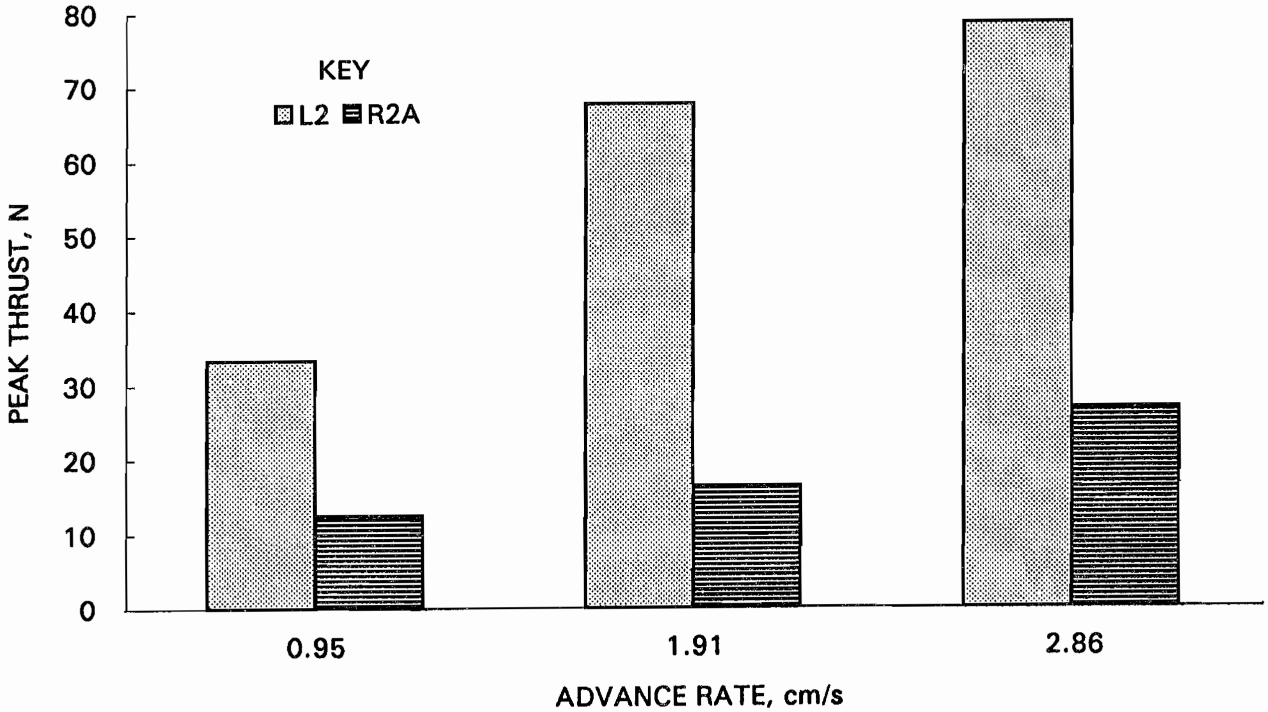

Peak thrust results for linear and slow rotary drum.

Figure 22

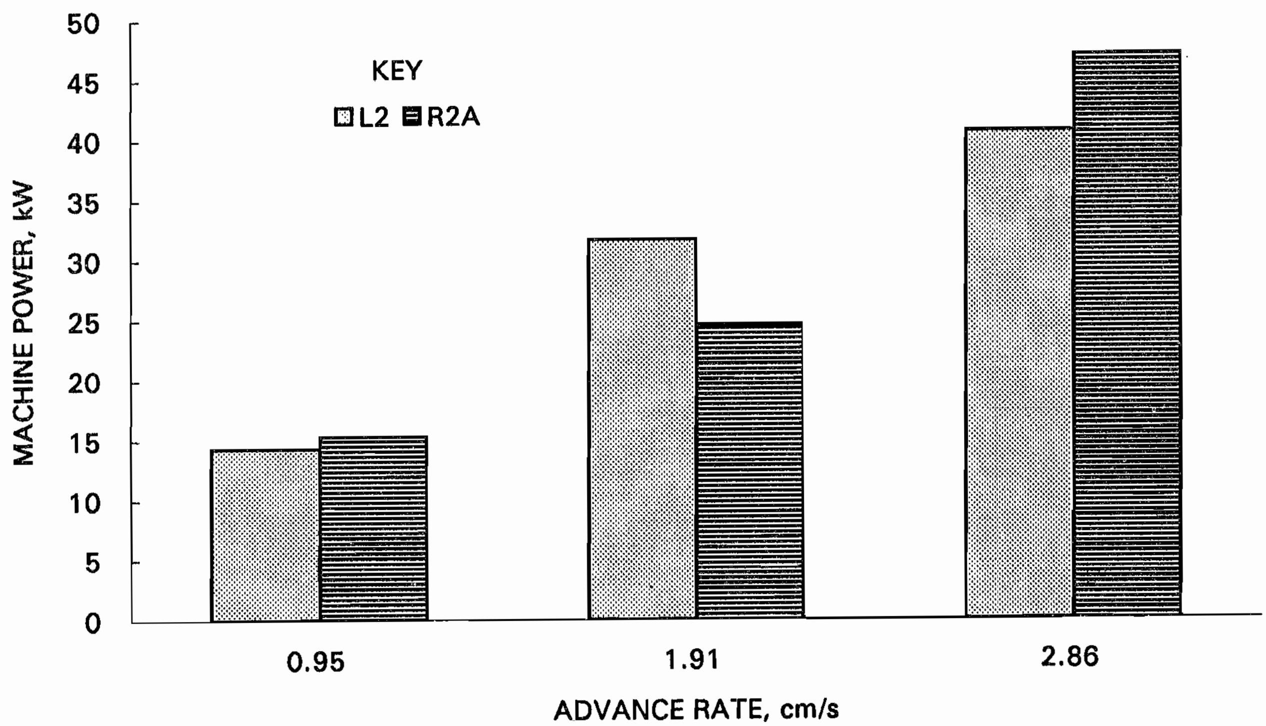

Power results for linear and slow rotary drum.

Figure 23

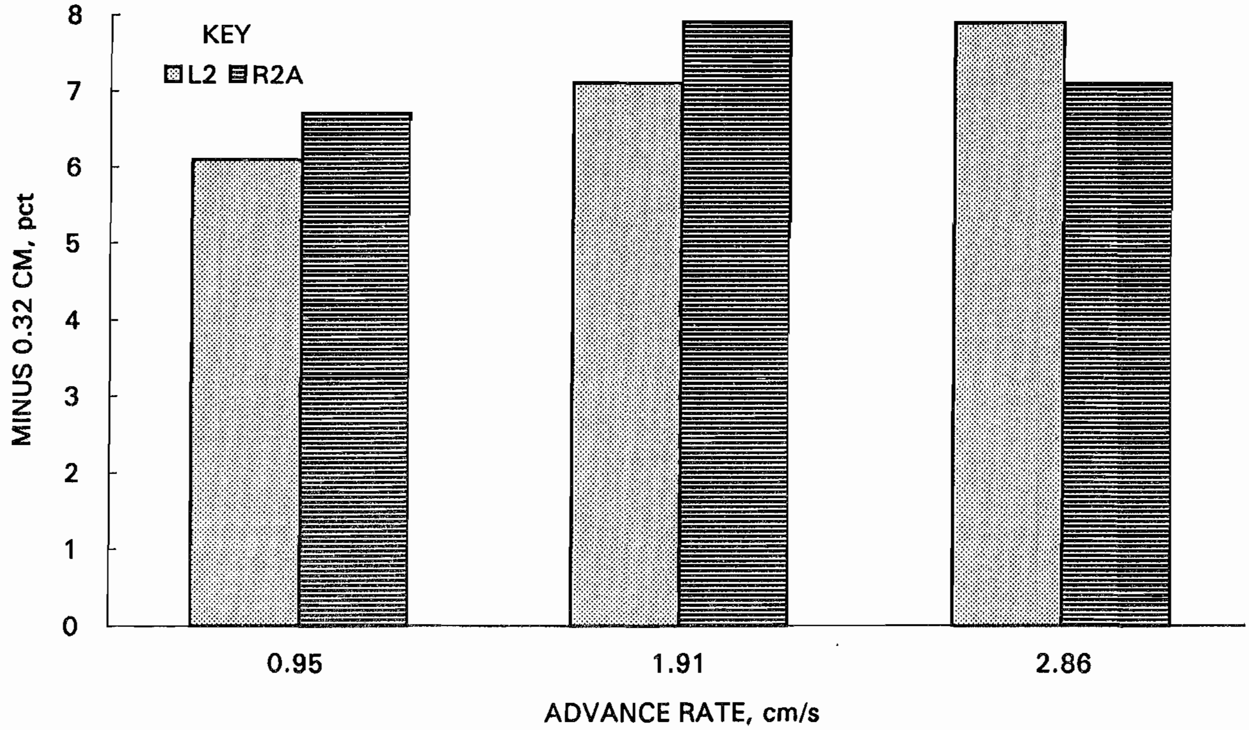

Results for minus 0.32 cm (1/8 in) for linear and slow rotary drum.

Figure 24

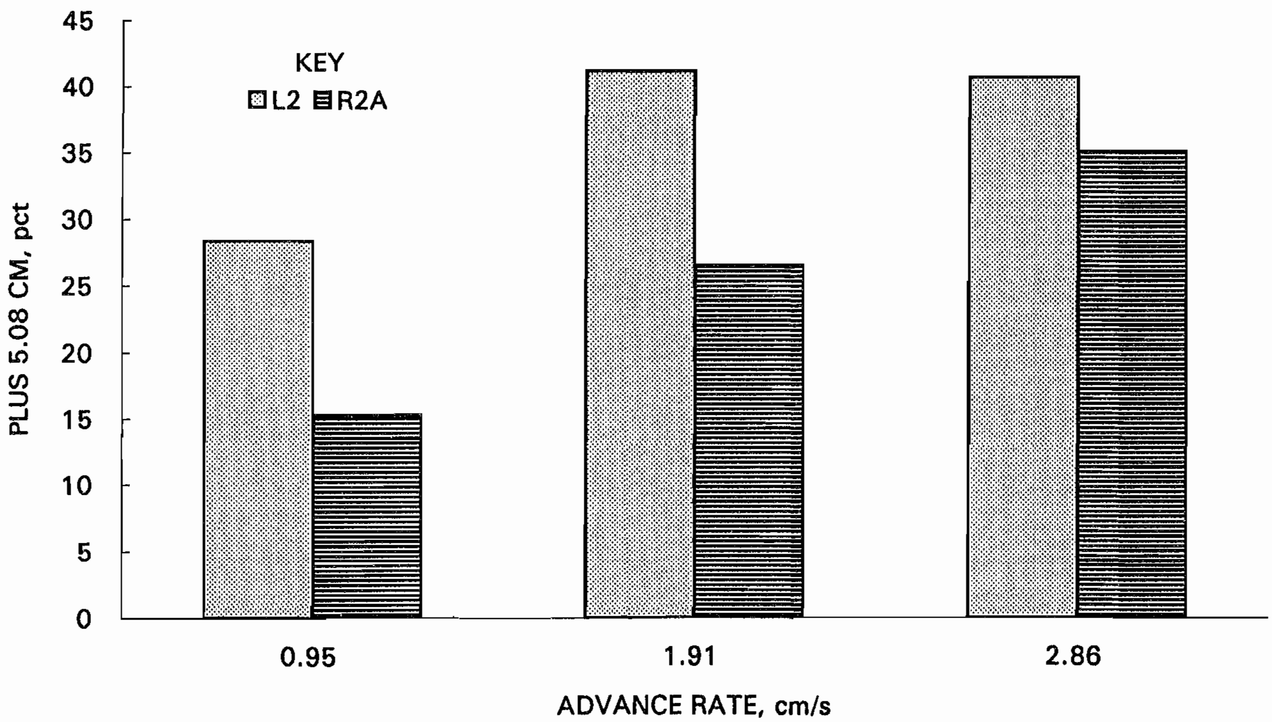

Results for plus 5.08-cm (2-in) material for linear and slow rotary drum.

Table 5.—Replicated test set

Variable	L2 drum	R2B drum	R4 drum
Specific dust, mg/m^3	0.028 ± 0.003	0.059 ± 0.004	0.092 ±
Average torque, N-m	6254 ± 244	6847 ± 438	0.007
Average thrust, kN	10.26 ± 1.87	4.58 ± 0.26	10005 ± 733
Power, kW	29.47 ± 1.12	35.88 ± 2.31	9.77 ± 0.13
Minus 0.32-cm product, pct	6.40 ± 0.7	9.45 ± 1.0	52.44 ± 3.88
Plus 5.08-cm product, pct	42.27 ± 1.0	6.83 ± 1.8	12.03 ± 1.3
			17.10 ± 0.9

Replicated Data

Table 5 and figure 25 show the portion of the experiment which was replicated. As can be seen by comparing figure 25 and figures 9-16, values for the three drums at the 1.91 cm/s (0.75 in/s) advance rate, the data were consistent.

STATISTICAL ANALYSIS

Both the data from the full factorial (five drum types and three advance rates) and the replicated tests were analyzed using standard analysis of variance techniques (ANOVA) (*9*). The summary of results (table 6) identifies parameters affected by drum type and/or advance rate for the full factorial.

With the exception of the minus 0.32-cm (1/8-in) mesh screen as a function of advance rate, all of the dependent variables showed a significant difference at a confidence level of 95 pct. The complete ANOVA tables are given in appendix D.

Table 6.—Analysis of variance results for five drums

	Specific dust	Torque	Thrust	Power	Minus 0.32-cm product	Plus 5.08-cm product
Full factorial:						
Drum ...	Yes	Yes	Yes	Yes	Yes	Yes
Advance rate ...	Yes	Yes	Yes	Yes	No	Yes
Replication:						
Drum ...	Yes	Yes	Yes	Yes	Yes	Yes

Note.—The yes or no in the table indicates the significance of the variable at the 95-pct level of confidence for each response.

Figure 25

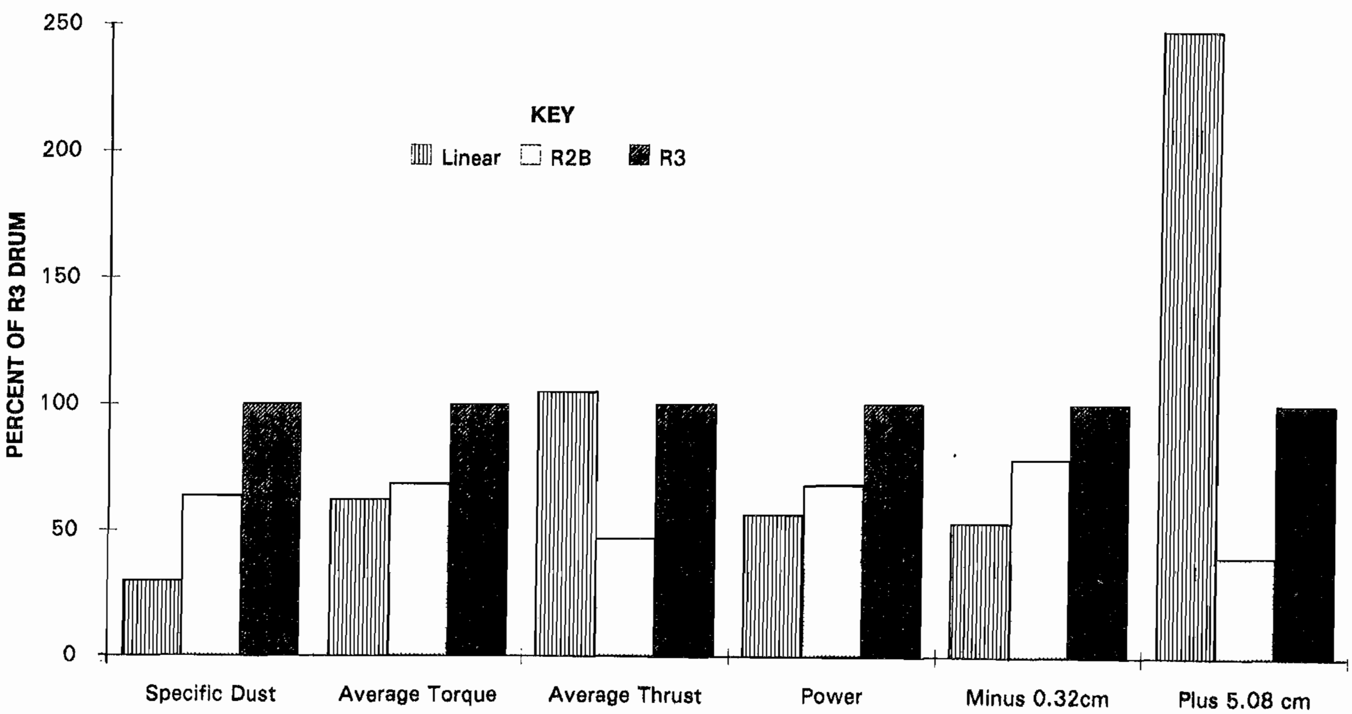

Replicated data.

CONCLUSIONS

Testing has confirmed the validity of the new linear cutting concept. Dust generation is reduced with linear cutting from 35 to 90 pct for the same production rate when the rotary drums are cutting relatively shallow and at high drum speeds. As depths of bit penetration of the rotary cutting increased due to slower drum speed to that used by the linear drum, dust generation levels were approximately the same. Linear cutting, with one exception, required less power than the rotary drum configurations. The maximum difference was 70 pct. Linear cutting consistently produced more +5.08-cm (+2-in) product than the rotary drums tested and produced the same or less, -0.32-cm (-1/8-in) product.

The mechanics of linear cutting required the development of a new eccentric drive system for the concept to become operational. The resulting high-torque gerotor gearbox, modified to accommodate rotary cutting, may provide the ability to cut slow and deep with a rotary drum machine. Past USBM research (*8*) has shown the potential benefits of such a system, but to date there is no gearbox capable of withstanding the strain imposed by such a cutting mode.

REFERENCES

1. Roepke, W. W., D. P. Lindroth, and J. W. Rasmussen. Linear Cutting Rotary Head Continuous Mining Machine. U.S. Pat. 4,025,077, Mar. 15, 1977.
2. Roepke, W. W., K. C. Strebig, and B. V. Johnson. Method of Operating a Constant Depth Linear Cutting Head on a Retrofitted Continuous Mining Machine. U.S. Pat. 4,025,116, May 25, 1977.
3. Roepke, W. W., D. P. Lindroth, and R. J. Wilson. Automatic Face Transfer by Linear Cutting Rotary Head. U.S. Pat. 4,062,595, Dec. 13, 1977.
4. Roepke, W. W., and S. J. Anderson. Triangular Shaped Cutting Head for Use With a Longwall Mining Machine. U.S. Pat. 4,303,277, Dec. 1, 1981.
5. Roepke, W. W., D. P. Lindroth, and T. A. Myren. Reduction of Dust and Energy During Coal Cutting Using Point Attack Bits With a Discussion of Rotary Cutting and Development of a New Cutting Concept. USBM RI 8185, 1976, 53 pp.
6. Courtney, W. G. New Development in Respirable Dust Control (Proc. Symp. on Underground Mining, Louisville, KY, Oct. 1975). NCA/BCR Coal Conf. and Expo II, pp. 103-109.
7. Matta, J. E. Effect of Location and Type of Water Sprays for Respirable Dust Suppression on a Continuous Mining Machine. USBM TPR 96, 1976, 11 pp.
8. Black, S., R. L. Schmidt, and B. V. Johnson. Reduced Generation of Airborne Dust Through Deep Cutting Continuous Miners. Coal Age, v. 82, No. 10, Oct. 1977, pp. 158-160.
9. Hicks, C. R. Fundamental Concepts in the Design of Experiments. Holt, Rinehart & Wilson, New York, NY, 1964, 293 pp.

APPENDIX A.—DESCRIPTION OF TEST FACILITY

GENERAL FACILITY DESCRIPTION

The Multibit Test (MBT) stand (figure A-1) was developed to verify the mechanics of the linear cutting concept and to allow comparisons between existing rotary cutting systems and the linear cutting system. It consists of a fixed drum mounting-drive system, a sample transport table and a control-measurement system. The MBT was built so that each drum cut a 76.2-cm-wide (30 in) by 81.3-cm-high (32 in) cross section, which is equivalent to a low-seam longwall shearer or to one-fourth of a continuous miner head on sump. The drums are mounted on a fixed support frame and the synthetic coal sample is moved perpendicular to the axis of the drum to simulate cutting an entry or panel. The cutting system drums were designed to be interchangeable on the test stand.

The sample transport is a heavy steel table mounted on cam rollers moved by a hydraulic cylinder. The maximum displacement of the sample transport table is 1.83 m (6 ft).

Two hydraulic pumps are used to drive the drum rotation and the sample transport table independently. The drum rotation system has a 74.6-kW (100-hp) electric motor driving a 378.5-L/min (100-gal/min) pump which operates a 74.6-kW (100-hp) hydraulic motor. With the gerotor gearbox, the linear drum can operate up to 15 rpm while any rotary drum without the gear reduction can operate up to 50 rpm. A 29.8-kW (40-hp) electric motor powers the hydraulic system used to move the sample transport table into the rotating drum. This system has two flow control valves giving two table speed ranges of 0.64 to 1.91 cm/s and 2.54 to 7.62 cm/s (0.25 to 0.75 in/s and 1.0 to 3.0 in/s), respectively.

FACILITY INSTRUMENTATION

Load-Position Measurements

The facility is equipped to measure both forces and position. Measurement-control functions include: sample

Figure A-1

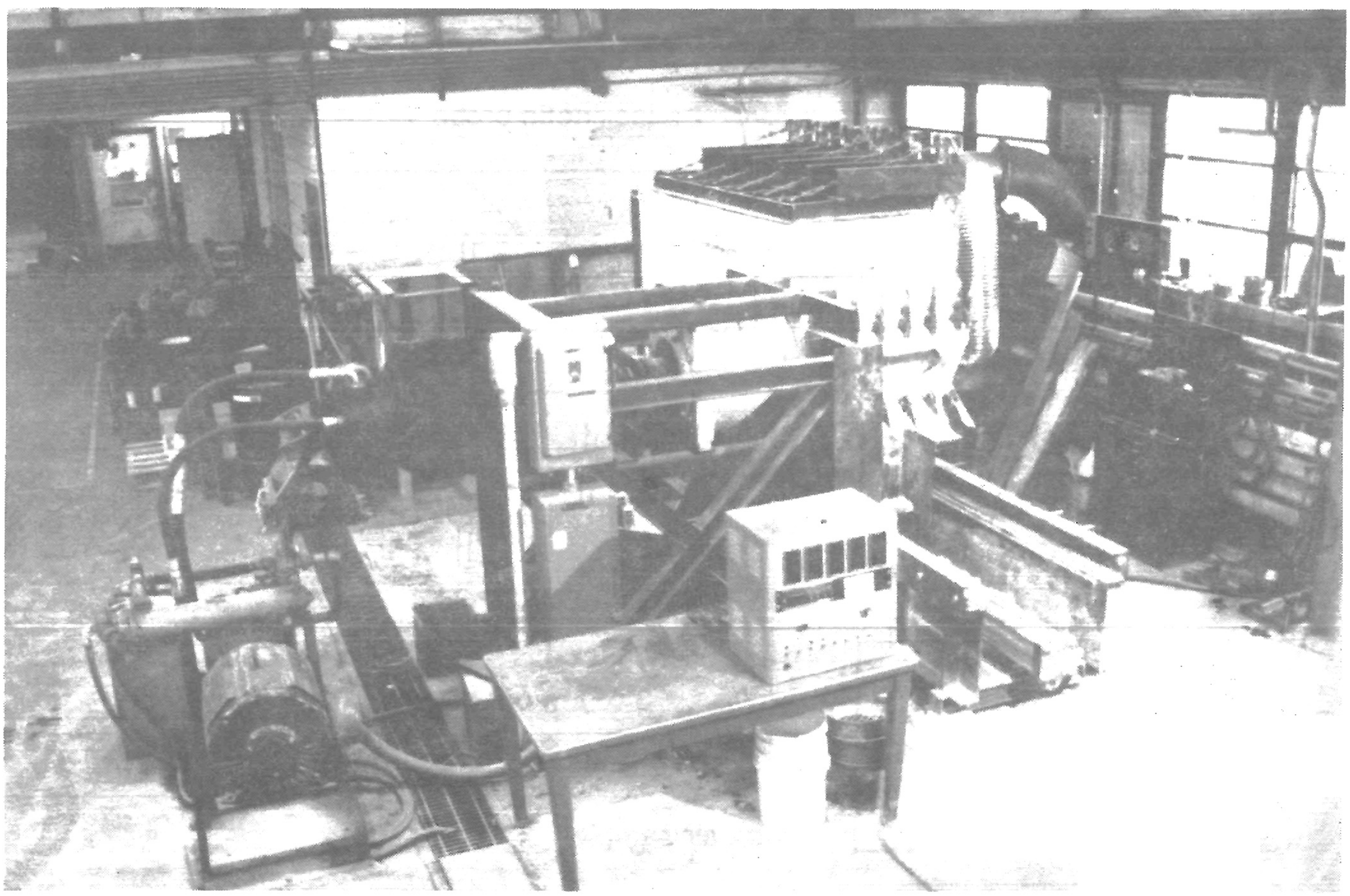

Mainframe of multibit test facility.

infeed thrust, sample position, drive-shaft torque, angular displacement of shaft, shaft revolution per minute, and infeed table speed. The latter two are provided to facilitate setting manual controls. The thrust transducer used is a commercially available strain-gauged clevis pin mounted in the hydraulic cylinder eye which fastens to the sample support table. Shaft torque measurements are implemented using strain gauge transducers mounted on the drive shaft. All torque values reported in this report are shaft torques. For rotary drums, the shaft torque and drum torques are equivalent. For the linear drum, drum torque is three times the measured shaft torque because of the three to one gear reduction in the gerotor.

All measurement channels are fed into a bank of signal conditioning modules which provide input offset, gain and transducer excitation, and analog light-emitting diode bar graph display of the output. The system has limit and overload controls to prevent system damage. The control system also has an override to allow the table or head to be backed out if it does become jammed. User-adjustable, vernier potentiometers on the hydraulic valves control the revolution per minute and table speeds.

Primary data acquisition is accomplished with a four-channel frequency modulation data tape recorder using standard 4.70 cm/s (1-7/8 in/s) tape cassettes. The tape is replayed through a low-pass filter into an analog-to-digital converter interfaced with a personal computer. Commercial data acquisition software digitize and store the test signals in a format that can then be directly imported into a spreadsheet for analysis.

Dust Measurement

A schematic of the dust measurement system is shown in figure A-2. The drum and sample table are enclosed in a dust shroud during testing. Dust liberated during a cutting test is entrained in the air of the test chamber. The dust-laden air is pulled from the test chamber through a 30.48-cm-diameter-exhaust (12 in) duct at 70.79 m^3/min (2,500 ft^3/min). An isokinetic sampling probe is located in this discharge duct. A 0.11-m^3/min (4-ft^3/min) constant flow air pump draws a sample of the aerosol through a 3.5-μm cut-point cyclone. The dust, smaller than 3.5 μm, is collected by the afterfilter. Gravimetric analysis is performed to determine the amount of dust collected on the afterfilter. The result is divided by the cubic feet of sample material removed to calculate a specific dust value.

Figure A-2

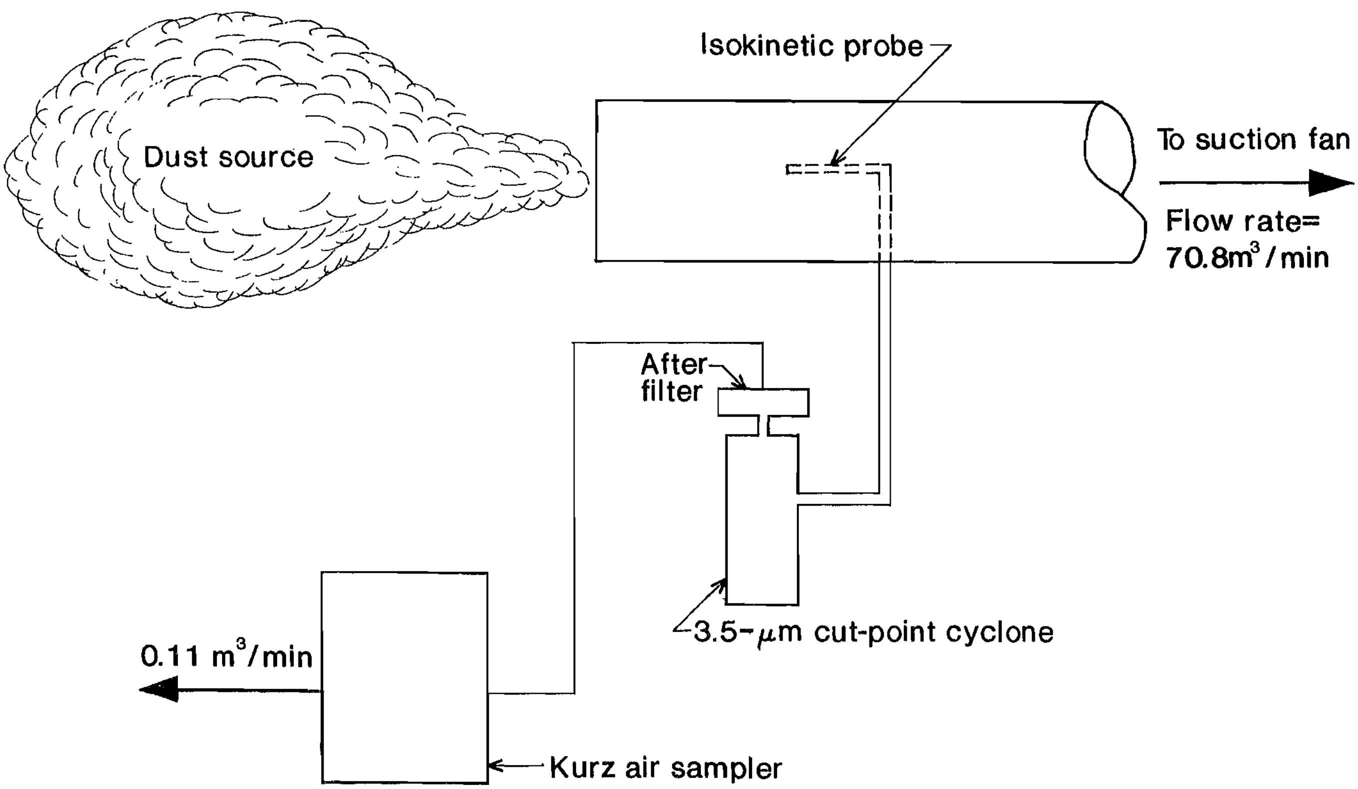

Schematic of dust measurement system.

SYNTHETIC COAL SAMPLE

Because coal disintegrates rapidly when exposed to air, and because it is difficult to obtain the quantity, size, and consistency needed for these tests, a synthetic coal sample is used in the cutting tests. This synthetic material is made from No. 1 molding plaster. With careful control of water content and curing times, the final test block reverts to gypsum which exhibits the same cutting forces as Illinois No. 6 coal. A comparison of cutting forces between the synthetic coal and Illinois No. 6 coal is shown in figure A-3. The average and peak tangential values are nearly identical, but the normal forces are slightly less in the simulated material. The synthetic coal does not have any internal fracturing or cleats as coal does. Although it fractures in a brittle manner and has nominally similar cutting forces, it is much tougher cutting than coal. Since all the drums were tested in the same material, the comparisons between them are valid.

The recipe for these gypsum blocks is 39.69-kg (87.5-lb), No. 1 molding plaster, 23.81-kg (52.5-lb) water, which is 60 pct of the plaster weight, and 7.09-g (1/4-oz) sodium citrate. After slow mixing to control aeration and voids, a 30-min cure in the mixing form is used for initial setup. They are then taken out of the form and placed in a low-temperature oven 43.3 °C ±2.8° (110 °F ±5°). After the blocks have been in the oven for 3 weeks, they have lost all free water, and the plaster has reverted to a gypsum with a weight of about 46.27 kg (102 lb). At this point, they are uniformly dry and ready for assembly into the large sample to make a simulated coal seam. The material in this dried condition is minimally hygroscopic so the blocks can be stored on open pallets (figure A-4), awaiting final use.

The cutting tests require a simulated coal seam with the approximate size of 0.91 by 1.22 by 2.13 m (3 by 4 by 7 ft). This large sample is made-up of 60 smaller blocks which are 30.48 by 30.48 by 41.91 cm (12 by 12 by 16-1/2 in). The 60 blocks are assembled using a Super X Hydrostone as a binder between blocks. The binder, which acts like shale bands in the seam, is more difficult to cut than the synthetic coal. A completed simulated seam with the roof steel bolted down on top and ready for test cuts is shown in figure A-5. Figures A-6 and A-7 show the simulated seam after test cuts using the rotary and linear drums, respectively.

Figure A-3

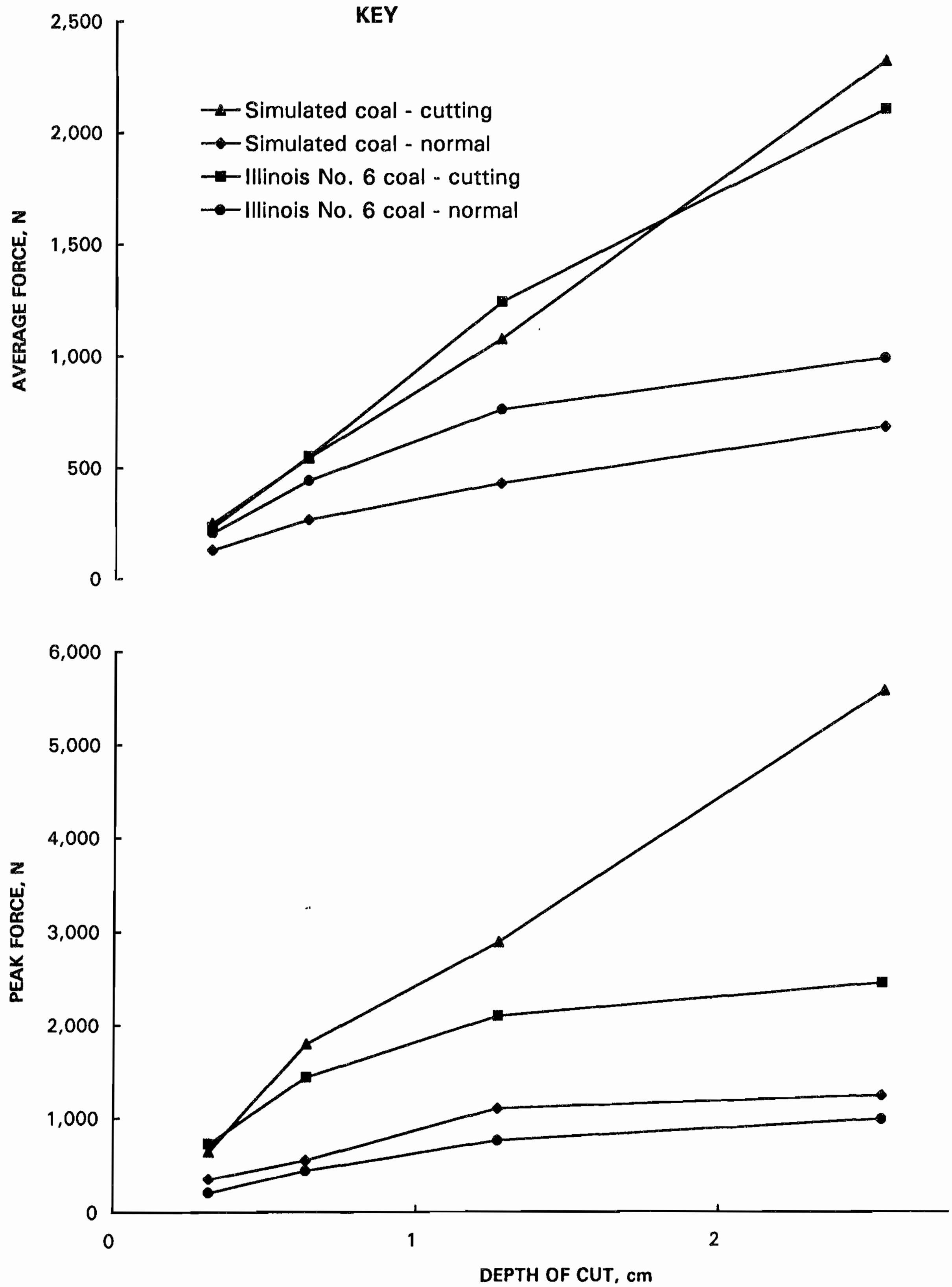

Comparison of Illinois No. 6 coal and simulated coal.

Figure A-4

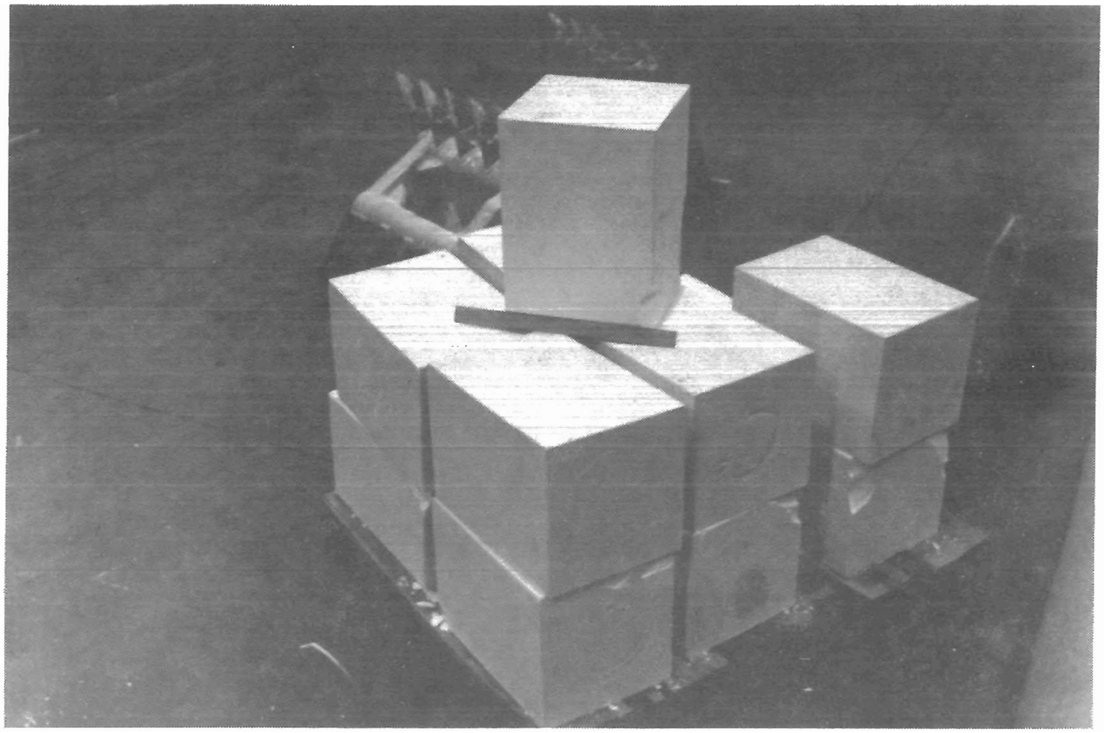

Pallet of simulated coal blocks in storage.

Figure A-5

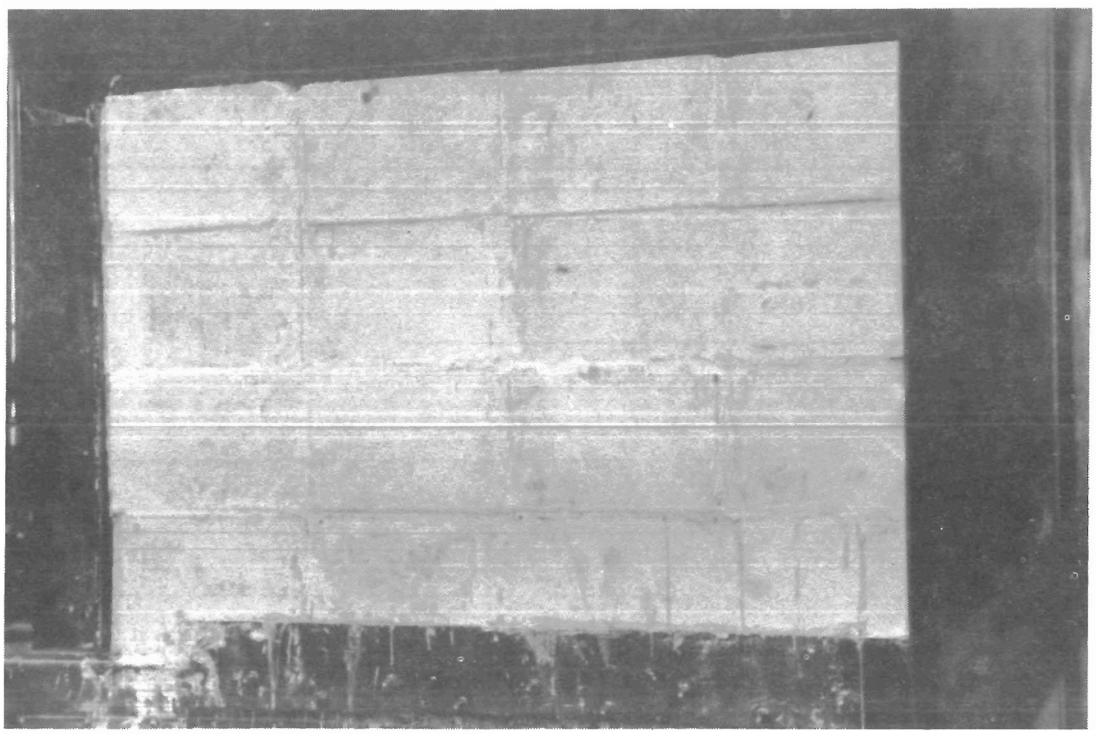

Assembled test sample ready for cutting test.

Figure A-6

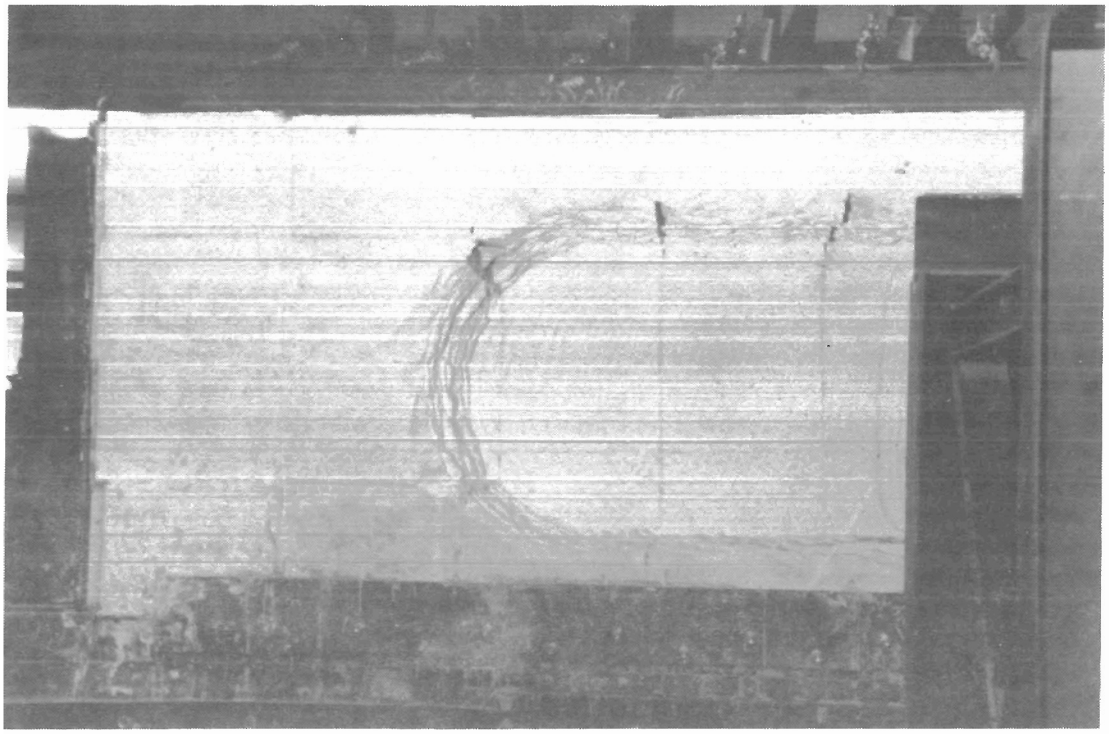

Shape of face after rotary cutting.

Figure A-7

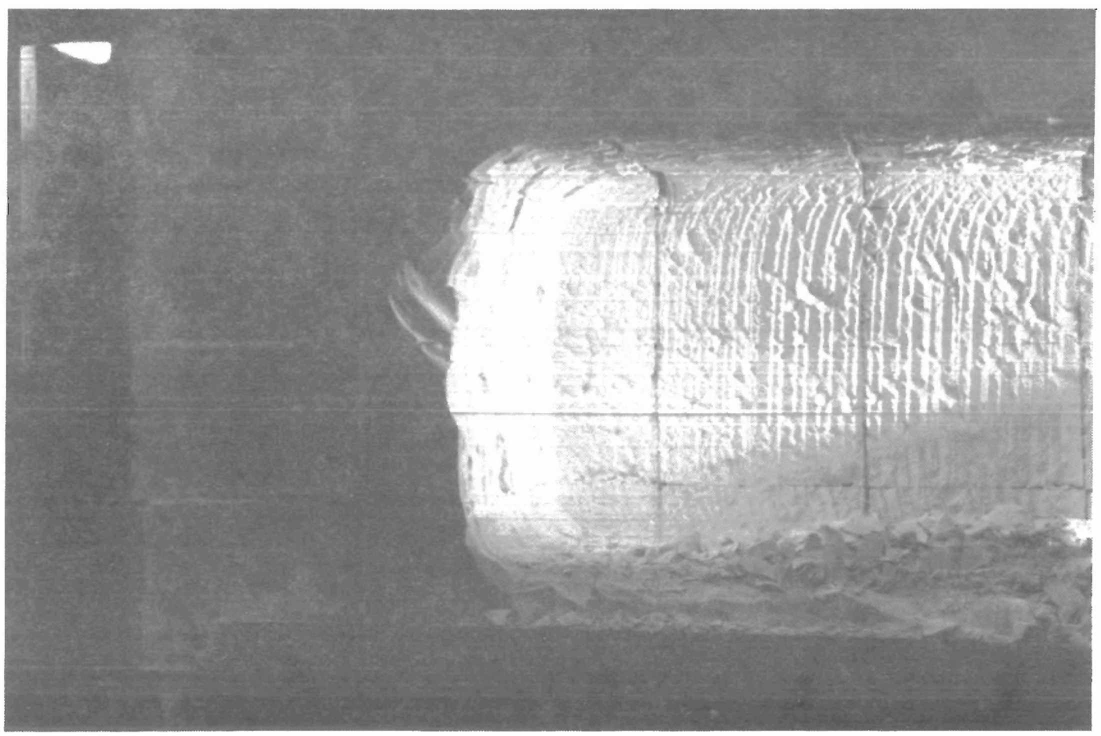

Shape of face after linear cutting.

APPENDIX B.—INDIVIDUAL TEST RESULTS

Table B-1.—Test results

Variable and drum	Advance rate, cm/s		
	0.95	1.91	2.86
Specific dust, mg/m^3:			
L2	0.035	0.033	0.026
R2A	0.050	0.013	0.009
R2B	0.072	0.050	0.059
R3	0.216	0.078	0.064
R4	0.262	0.159	0.104
Average torque, N-m:			
L2	3,030	6,721	8,624
R2A	6,507	10,434	19,940
R2B	7,153	8,161	7,014
R3	11,263	11,404	13,695
R4	9,291	10,730	13,557
Peak torque, N-m:			
L2	6,4591	10,798	16,358
R2A	1,726	16,320	20,873
R2B	10,723	15,161	10,691
R3	17,704	18,066	20,218
R4	17,965	20,203	21,246
Average thrust, kN:			
L2	4.27	10.44	13.78
R2A	4.29	6.27	8.01
R2B	4.29	4.83	4.66
R3	11.80	9.98	12.24
R4	12.47	15.50	18.62
Peak thrust, kN:			
L2	33.4	67.7	78.5
R2A	12.5	16.3	26.8
R2B	10.5	12.1	9.7
R3	23.0	24.0	29.4
R4	27.0	26.5	27.6
Power, kW:			
L2	14.3	31.7	40.6
R2A	15.3	24.6	47.0
R2B	37.5	42.7	36.7
R3	59.0	59.7	71.7
R4	48.7	56.2	71.0
Minus 0.32-cm, pct:			
L2	6.1	7.1	7.9
R2A	6.7	7.9	7.1
R2B	19.8	12.4	7.5
R3	24.3	14.7	11.8
R4	17.8	11.9	10.2
Plus 5.08-cm, pct:			
L2	28.4	41.2	40.7
R2A	15.3	26.6	35.1
R2B	8.3	10.3	13.4
R3	18.8	15.8	23.1
R4	11.0	8.3	19.7

Table B-2.—Maximum cut depth of test drums

Drum type	Advance rate, cm/s		
	0.95	1.91	2.86
L2	1.27	2.54	3.81
R2A	1.27	2.54	3.81
R2B	0.58	1.14	1.73
R3	0.58	1.14	1.73
R4	0.38	0.76	1.14

Note.—For the linear drum, L2, the average cut depth is 84 pct of the maximum. For the rotary drums, R2A through R4, the average cut depth is 67 pct of the maximum.

APPENDIX C.—BIT FORCE DETERMINATIONS

General Comments on Bit Forces

Based on past experience, direct bit force measurements were considered to be impractical. The test stand instrumentation does, however, allow the measured values of shaft torque, shaft angle, and sample advance to be used to determine average forces on the bits. A brief discussion of these bit force determinations and a summary of their calculated values are presented in this appendix for the linear tests.

Discussion of Bit Force Determination

The resultant force fed through the tip of the bit is resolved into two components, normal and tangential. The normal force is defined as the component of the resultant force which is directed along a line originating at the axis of rotation and terminating at the bit tip. The tangential force is defined as the component of the resultant force which is directed along a line perpendicular to the normal force. The tangential force vector, as its name implies, is always tangent to the locus of the bit tip as it proceeds through the cutting cycle.

Torque at the measurement point (drive shaft) is transformed into head torque and then divided by the moment arm length, (the distance from the center of rotation to the bit tip) to get tangential force. The normal force is determined by summing the projections of the normal and tangential force vectors onto the horizontal axis and equating this sum to the sample infeed thrust and finally solving the equation for the unknown quantity (normal force). The measured quantities that are input to the transformation equations are shaft angle, shaft torque and sample infeed thrust. The accuracy of the transformation equations is dependent on the accuracy of the values for the measured quantities as well as the angular position of the head or shaft. As the direction of the normal force vector increases beyond 45°, the equations for normal force become increasingly sensitive to errors in the independent variables (measured quantities). This is intuitively obvious since, as the normal force vector approaches a vertical position, the projection of that vector onto the horizontal axis is approaching zero. The following provides some of the details including the transformation equations (without derivations) pertaining to the bit force calculations for each specific cutting system.

Linear Cutting Specifics

The transformation equations are complicated due to the fact that the moment arm, r, is not a constant, but varies with shaft angle and also that the relationship between shaft torque and head torque is dependent on the geometry of the gerotor assembly. A schematic representation of the linear head and gerotor is provided by figure C-1. Identified in the construction and relevant to this discussion are the moment arm, r; the gerotor to bit tip distance, l; the ring radius, a; the gerotor radius, b; the normal force, FN; the tangential force, FT; the shaft angle, θ; and the normal force vector direction, α. The tangential force, FT, is expressed in terms of the shaft torque, T, the shaft torque transformation ratio, b/(a-b), and the moment arm length, r, by:

$$FT = \frac{Tb}{r(a-b)}, \tag{1}$$

The value of r is given by the rather complicated expression shown below in equation 2.

The expression for normal force is obtained by equating the sum of the projections of the vectors FT and FN onto the horizontal axis to the sample infeed thrust FX and solving for FN to get:

$$FN = \frac{FX - FT\sin\alpha}{\cos\alpha} \tag{3}$$

The angle, α, can be expressed in terms of the shaft angle, θ, by:

$$\alpha = \arctan \frac{-l\sin\left(\frac{\pi - \theta}{3}\right) + b\sin\theta}{-l\cos\left(\frac{\pi - \theta}{3}\right) + b\cos\theta} \tag{4}$$

Linear Bit Forces

Bit forces have been calculated for each pass (each row of bits) of each linear cutting test. The calculated values are based on torque and thrust values sampled every 50 ms. A separate angle transducer measures shaft angle since that is the independent variable in the transformation equations. Bit force data versus shaft angle for a typical cut of a bit row on the linear drum from the top corner to the bottom corner of the face are shown in figure C-2. The force values given in figure C-2 are distributed equally over the bits (five or six for drum L2) in the row along any single apex of the linear drum. Although the cutting cycle ranges from 0° to 360° of shaft angle, the transformation equations are useful only over the range of approximately 45° to 315° of shaft angle (top corner to bottom corner).

$$r = \sqrt{\left[l\cos\left(\frac{\pi - \theta}{3}\right) + (a - b)\cos\theta - a\cos\theta\right]^2 + \left[l\sin\left(\frac{\pi - \theta}{3}\right) + (a - b)\sin\theta - a\sin\theta\right]^2} \tag{2}$$

Outside of this range, normal force determinations are excessively sensitive to measurement errors in torque and thrust. For this reason, in figure C-2, tangential force includes the corners while the normal force is shown for only the linear portion of the cut. An increased tangential force about shaft angles of 45° and 315° may be seen at the upper and lower corners. At the midface point, where the row of bits is encountering an inclusive shale band, (layer of hydrostone cement), a peak may also be seen in the tangential force. There is a peak in the normal force at a shaft angle of 90° which corresponds to the beginning of the linear portion of the cut. These are features typical of all of the linear test data. A summary of the bit force data from the second-generation linear drum, L2, cutting tests reported in this document are shown in figure C-3. This figure shows the calculated single-bit forces, averaged over the linear portion of the face being cut, for the three advance rates used. The average peak normal and tangential forces for the upper corner region are also shown. The average and peak normal forces are relatively low, and insensitive to depth, over the range of advance rates covered by these tests. This is consistent with past experience in linear cutting when using this bit geometry. Peak tangential force is more sensitive to depth of cut and is significantly higher in magnitude than is the average tangential force over the linear range. A mitigating factor is the tangential force capability of the system. The tangential force capability varies over the cutting cycle as shown in figure C-4. The tangential force capability for a given shaft torque is 2.2 times greater in the corner than at the midface point because the length of the moment arm (the distance from the instantaneous center of rotation to the bit tip) varies as a function of shaft angle and length of the eccentric arm. The angle of attack of the bit (defined as the angle lying between the centerline of the bit and the normal force direction) also varies with shaft angle as shown in figure C-5. Notice that the angle of attack in the corners (shaft angle at 45° and 315°) is equal to the angle of attack at the midface point. This identifies one of the significant differences between linear and rotary cutting systems. The linear cutting system has a constantly varying angle of attack with a fixed depth of cut across the linear portion of the face. Rotary drum systems use a fixed angle of attack with a constantly varying depth of cut across the face.

Figure C-1

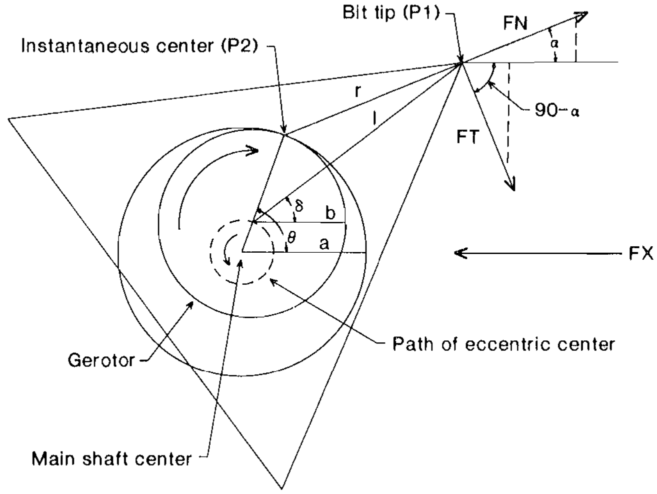

Bit force vector schematic for linear drum.

Figure C-2

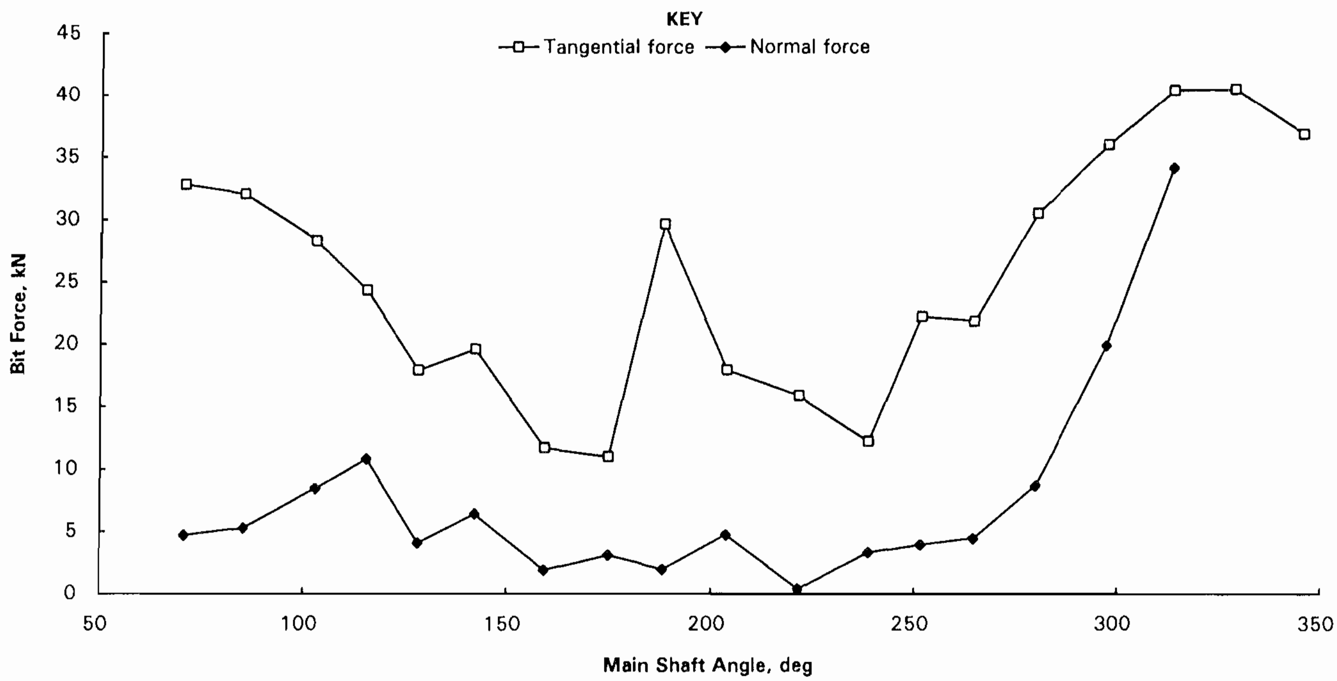

Tangential and normal force versus shaft angle.

Figure C-3

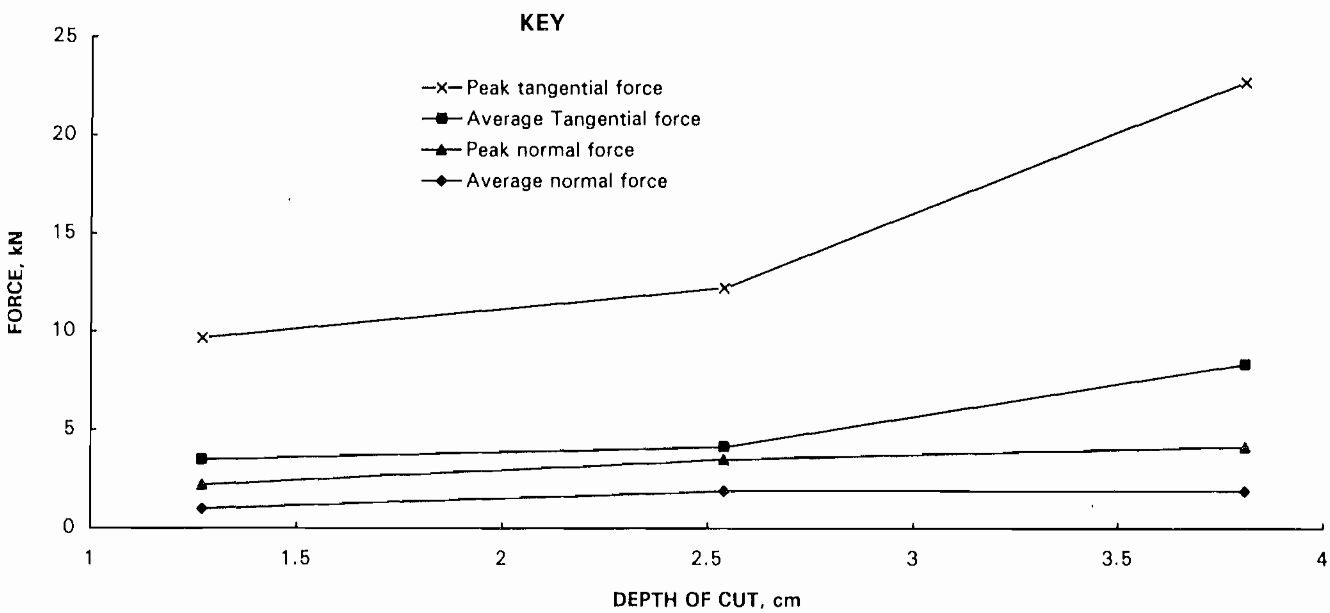

Bit force versus depth of cut for L2.

Figure C-4

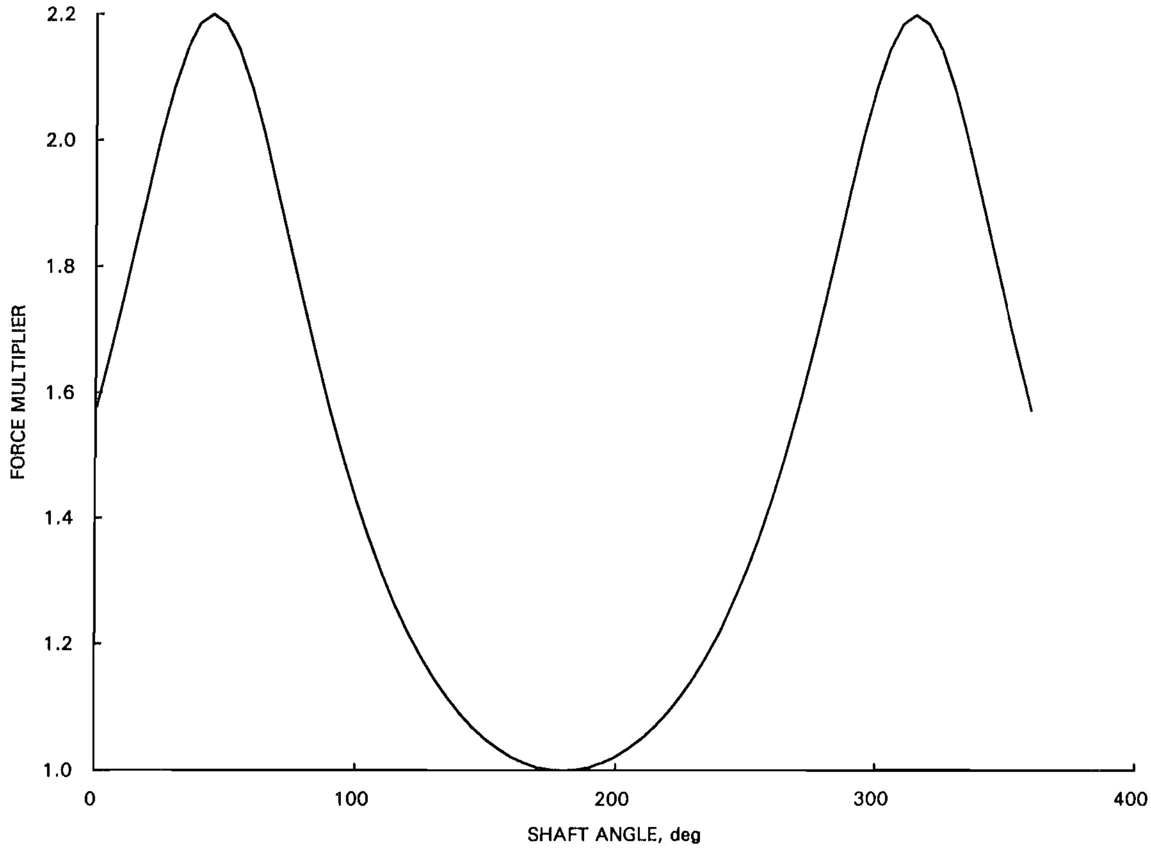

Tangential force capability versus shaft angle.

Figure C-5

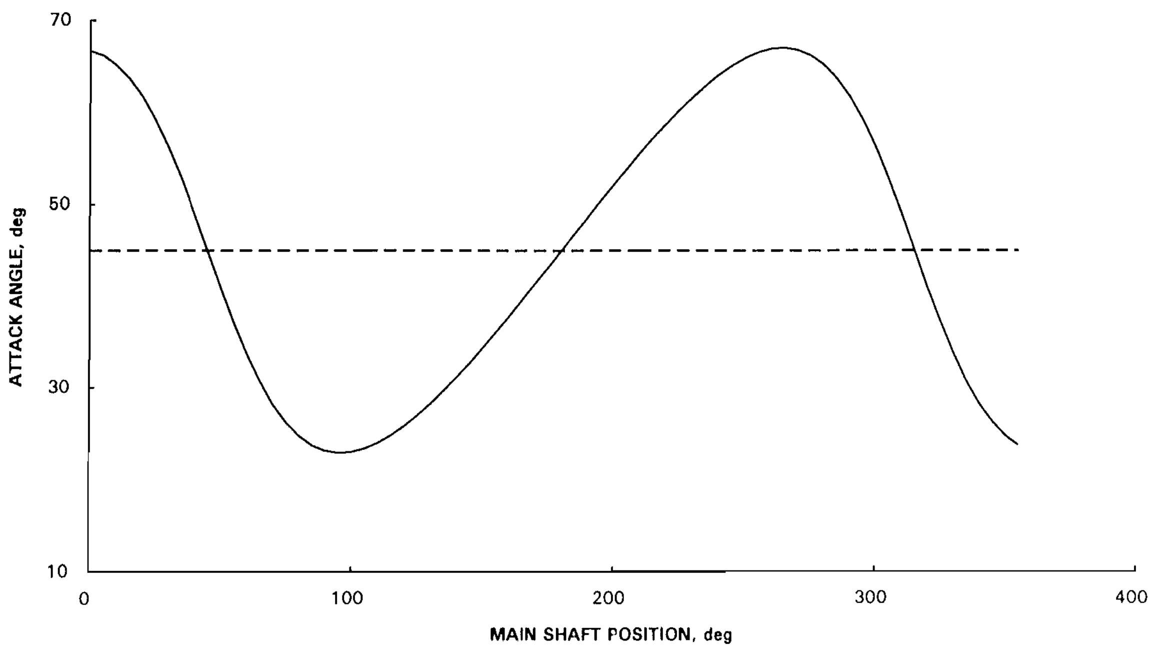

Variation in bit attack angle across face during linear cutting.

APPENDIX D.—ANALYSIS OF VARIANCE

The ANOVA results for a full factorial with no replication for the experimental series using five different drums and three different advance rates are shown in tables D-1 and D-2. Tables D-3 through D-4 show the ANOVA results for the experimental series where three and four replications were made using three drums at an advance rate of 1.91 cm/s (0.75 in/s).

Table D-1.—Test results for full factorial experiment

Variable and drum	Advance rate, cm/s		
	0.95	1.91	2.86
Specific dust, mg/m^3:			
L2	43.5	40.5	32.8
R2A	62.8	15.8	11.6
R2B	89.7	62.3	73.1
R3	269.2	97.7	79.9
R4	326.9	198.8	129.5
Average thrust, kN:			
L2	4.27	10.44	13.78
R2A	4.29	6.27	8.01
R2B	4.29	4.83	4.66
R3	11.80	9.98	12.24
R4	12.47	15.50	18.62
Peak thrust, kN:			
L2	33.4	67.7	78.5
R2A	12.5	16.3	26.8
R2B	10.5	12.1	9.7
R3	23.0	24.0	29.4
R4	27.0	26.5	27.6
Average torque, N-m:			
L2	3,030	6,721	8,624
R2A	6,506	10,434	19,940
R2B	7,153	8,161	7,014
R3	11,263	11,404	13,695
R4	9,291	10,730	13,557
Peak torque, N-m:			
L2	6,459	10,798	16,358
R2A	11,726	16,320	20,873
R2B	10,723	15,161	10,691
R3	17,704	18,066	20,218
R4	17,965	20,203	21,246
Power, kW:			
L2	14.3	31.7	40.6
R2A	15.3	24.6	47.0
R2B	37.5	42.7	36.7
R3	59.0	59.7	71.7
R4	48.7	56.2	71.0
Minus 0.32-cm screen size, pct:			
L2	6.1	7.1	7.9
R2A	6.7	7.9	7.1
R2B	19.8	12.4	7.5
R3	24.3	14.7	11.8
R4	17.8	11.9	10.2
Plus 5.08-cm screen size, pct:			
L2	28.4	41.2	40.7
R2A	15.3	26.6	35.1
R2B	8.3	10.3	13.4
R3	18.8	15.8	23.1
R4	11.0	8.3	19.7

Table D-2.—ANOVA results for full factorial experiment

	Sum of squares	Mean square	F-value
Specific dust:			
Drum	7.69e+04	1.92e+04	7.86
Advance rate	2.44e+04	1.22e+04	4.99
Error	1.96e+04	2.45e+03	
Average thrust:			
Drum	224.33	56.08	12.93
Advance rate	40.79	20.39	4.70
Error	34.70	4.34	
Peak thrust:			
Drum	4.22e+03	1.06e+03	10.44
Advance rate	4.39e+02	2.20e+02	2.17
Error	8.09e+02	1.01e+02	
Average torque:			
Drum	9.78e+07	2.44e+07	3.31
Advance rate	6.64e+07	3.32e+07	4.49
Error	5.92e+07	7.40e+06	
Peak torque:			
Drum	1.75e+08	4.39e+07	6.97
Advance rate	6.32e+07	3.16e+07	5.02
Error	5.04e+07	6.30e+06	
Power:			
Drum	3.22e+03	8.04e+02	15.57
Advance rate	8.58e+02	4.29e+02	8.30
Error	4.13e+02	5.17e+01	
Minus 0.32-cm product:			
Drum	221.73	55.43	4.39
Advance rate	95.39	47.69	3.77
Error	101.10	12.64	
Plus 5.08-cm product:			
Drum	1.33e+03	3.33e+02	16.80
Advance rate	2.55e+02	1.27e+02	6.43
Error	1.58e+02	1.98e+01	

Table D-3.—Test results for replicated experiment

Variable and replication	Drum L2	Drum R2B	Drum R3
Specific dust, mg/m^3:			
1	29.6	66.5	122.1
2	33.5	62.3	97.7
3	40.5	81.2	126.0
4		84.4	
Average torque, N•m:			
1	6,143	6,463	9,688
2	5,897	8,161	11,404
3	6,721	6,390	8,923
4		6,376	
Peak torque, N•m:			
1	12,349	8,435	14,431
2	10,932	15,161	18,066
3	10,798	8,760	14,612
4		7,075	
Average thrust, kN:			
1	13.41	5.14	9.80
2	6.93	4.83	9.98
3	10.44	4.43	9.52
4		3.93	
Peak thrust, kN:			
1	71.46	10.01	21.23
2	52.44	12.14	24.05
3	67.69	8.69	21.67
4		8.56	
Power, kW:			
1	28.95	33.84	50.73
2	27.79	42.73	59.71
3	31.67	33.46	46.72
4		33.39	
Mean 0.32-cm product, pct:			
1	44.2	4.2	16.8
2	41.5	10.3	15.8
3	41.2	9.4	18.7
4		3.4	
Plus 5.08-cm product, pct:			
1	5.1	8.4	11
2	7	12.4	14.7
3	7.1	8.1	10.4
4		8.9	

Table D-4.—ANOVA results for replicated experiment

	Sum of squares	Mean square	F-value
Specific dust:			
Drum type	9.79e+03	4.90e+03	38.93
Error	8.80e+02	1.26e+02	
Average torque:			
Drum type	2.50e+07	1.25e+07	14.89
Error	5.89e+06	8.41e+05	
Peak torque:			
Drum type	6.07e+07	3.03e+07	4.34
Error	4.90e+07	7.00e+06	
Average thrust:			
Drum type	7.12e+01	3.56e+01	11.37
Error	2.19e+01	3.13e+00	
Peak thrust:			
Drum type	5.24e+03	2.62e+03	85.06
Error	2.16e+02	3.08e+01	
Power:			
Drum type	8.50e+02	4.25e+02	18.63
Error	1.60e+02	2.28e+01	
Minus 0.32-cm product:			
Drum type	2.21e+03	1.10e+03	164.01
Error	4.71e+01	6.73e+00	
Plus 5.08-cm product:			
Drum type	4.77e+01	2.39e+01	6.60
Error	2.53e+01	3.62e+00	

INT.BU.OF MINES,PGH.,PA 30061
☆ U S G P O 1995-609-012/ 20 002